

See discussions, stats, and author profiles for this publication at: <https://www.researchgate.net/publication/327176156>

Mitochondrial respiratory states and rates: Building blocks of mitochondrial physiology Part 1

Preprint · August 2018

CITATIONS

0

READS

841

8 authors, including:



Alice P. Sowton

University of Cambridge

5 PUBLICATIONS 2 CITATIONS

[SEE PROFILE](#)



María Huete-Ortega

Oroboros Instruments

56 PUBLICATIONS 491 CITATIONS

[SEE PROFILE](#)



Giovanna Distefano

AdventHealth

30 PUBLICATIONS 502 CITATIONS

[SEE PROFILE](#)



Rob C I Wüst

Vrije Universiteit Amsterdam

57 PUBLICATIONS 852 CITATIONS

[SEE PROFILE](#)

Some of the authors of this publication are also working on these related projects:



Smoking and skeletal muscle function [View project](#)



Oxygen supply and utilization in skeletal muscle [View project](#)



1
2
3 **Mitochondrial respiratory states and rates:**
4 **Building blocks of mitochondrial physiology Part 1**
5

6 **COST Action CA15203 MitoEAGLE preprint Version: 2018-10-25(45)**
7

8 Corresponding author: Gnaiger E

9 Co-authors:

10 Aasander Frostner E, Abumrad NA, Acuna-Castroviejo D, Adams SH, Ahn B, Ali SS, Alves MG,
11 Amati F, Amoedo ND, Andreadou I, Arago Belenguer M, Aral C, Arandarčikaitė O, Armand AS,
12 Arnould T, Avram VF, Bailey DM, Bajpeyi S, Bajzikova M, Bakker BM, Bastos Sant'Anna Silva AC,
13 Battino M, Bazil J, Beard DA, Bednarczyk P, Bello F, Ben-Shachar D, Bergdahl A, Berge RK,
14 Bergmeister L, Bernardi P, Bishop D, Blier PU, Blindheim DF, Boardman NT, Boetker HE, Boros M,
15 Borsheim E, Borutaitė V, Bouillaud F, Bouitbir J, Boushel RC, Bovard J, Breton S, Brown DA,
16 Brown GC, Brown RA, Brozinick JT, Buettner GR, Burtscher J, Calabria E, Calbet JA, Calzia E,
17 Cannon DT, Cano Sanchez M, Canto AC, Cardoso LHD, Carvalho E, Casado Pinna M, Cassina AM,
18 Castro L, Cavalcanti-de-Albuquerque JP, Cervinkova Z, Chabi B, Chakrabarti L, Chaurasia B, Chen
19 Q, Chicco AJ, Chinopoulos C, Chowdhury SK, Cizmarova B, Clementi E, Coen PM, Coker RH,
20 Collin A, Crisóstomo L, Dahdah N, Dambrova M, Danhelovska T, Darveau CA, Das AM, Dash RK,
21 Davidova E, Davis MS, De Goede P, De Palma C, Dembinska-Kiec A, Detraux D, Devaux Y, Di
22 Marcello M, Dias TR, Distefano G, Doermann N, Doerrier C, Donnelly C, Drahota Z, Dubouchaud H,
23 Duchen MR, Dumas JF, Durham WJ, Dymkowska D, Dyrstad SE, Dyson A, Dzialowski EM, Ehinger
24 J, Elmer E, Endlicher R, Engin AB, Escames G, Ezrova Z, Falk MJ, Fell DA, Ferdinandy P, Ferko M,
25 Ferreira JCB, Ferreira R, Fessel JP, Filipovska A, Fisar Z, Fischer C, Fischer M, Fisher G, Fisher JJ,
26 Ford E, Fornaro M, Galina A, Galkin A, Galli GL, Gan Z, Ganetzky R, Garcia-Roves PM, Garcia-
27 Souza LF, Garipi E, Garlid KD, Garrabou G, Garten A, Gastaldelli A, Genova ML, Giovarelli M,
28 Gonzalez-Armenta JL, Goncalo Teixeira da SR, Gonzalo H, Goodpaster BH, Gorr TA, Gourlay CW,
29 Granata C, Grefte S, Guarch ME, Gueguen N, Gumeni S, Haas CB, Haavik J, Haendeler J, Hamann A,
30 Han J, Han WH, Hancock CR, Hand SC, Handl J, Hargreaves IP, Harper ME, Harrison DK,
31 Hausenloy DJ, Heales SJR, Heiestad C, Hellgren KT, Hepple RT, Hernansanz-Agustin P, Hickey AJ,
32 Hoel F, Holland OJ, Holloway GP, Hoppel CL, Hoppel F, Houstek J, Huete-Ortega M, Hyrossova P,
33 Iglesias-Gonzalez J, Irving BA, Isola R, Iyer S, Jackson CB, Jadiya P, Jang DH, Jang YC, Janowska J,
34 Jansen K, Jansen-Dürr P, Jansone B, Jarmuszkiewicz W, Jaskiewicz A, Jespersen NR, Jha RK,
35 Jurczak MJ, Jurk D, Kaambre T, Kaczor JJ, Kainulainen H, Kampa RP, Kandel SM, Kane DA,
36 Kappler L, Karabatsiakakis A, Karkucinska-Wieckowska A, Keijer J, Keller MA, Keppner G, Khamoui
37 AV, Kidere D, Kilbaugh T, Klepinin A, Klingenspor M, Komlodi T, Koopman WJH, Kopitar-Jerala
38 N, Kowaltowski AJ, Kozlov AV, Krajcova A, Krako Jakovljevic N, Kristal BS, Kuang J, Kucera O,
39 Kuka J, Kwak HB, Kwast K, Laasmaa M, Labieniec-Watala M, Lai N, Land JM, Lane N, Laner V,
40 Lanza IR, Larsen TS, Lavery GG, Lazou A, Lee HK, Leeuwenburgh C, Lemieux H, Lenaz G, Lerfall
41 J, Li PA, Li Puma L, Liepins E, Liu J, Lucchinetti E, Ma T, Macedo MP, MacMillan-Crow LA,
42 Majtnerova P, Makarova E, Makrečka-Kuka M, Malik AN, Markova M, Marstein H, Martins AD,
43 Martin DS, Martins JD, Mazat JP, McKenna HT, Menze MA, Merz T, Meszaros AT, Methner A,
44 Michalak S, Moellering DR, Moiso N, Molina AJA, Montaigne D, Moore AL, Moreau K, Moreno-
45 Sánchez R, Moreira BP, Mracek T, Muntane J, Muntean DM, Murray AJ, Musiol E, Myhre Pedersen
46 T, Nair KS, Nehlin JO, Nemeč M, Neuffer PD, Neuzil J, Nevriere R, Newsom S, Nozickova K, O'Brien
47 KA, O'Gorman D, Olgar Y, Oliveira MF, Oliveira MT, Oliveira PF, Oliveira PJ, Orynbayeva Z,
48 Osiewicz HD, Ounpuu L, Pak YK, Pallotta ML, Palmeira CM, Parajuli N, Passos JF, Passrucker M,

49 Patel HH, Pavlova N, Pecina P, Pelnena D, Pereira da Silva Grilo da Silva F, Perez Valencia JA, Pesta
 50 D, Petit PX, Pettersen IKN, Pichaud N, Piel S, Pietka TA, Pino MF, Pirkmajer S, Porter C, Porter RK,
 51 Pranger F, Prochownik EV, Pulinilkunnil T, Puskarich MA, Puurand M, Quijano C, Radenkovic F,
 52 Radi R, Ramzan R, Rattan S, Reboredo P, Rich PR, Renner-Sattler K, Rial E, Robinson MM, Roden
 53 M, Rodríguez-Enriquez S, Rohlena J, Rolo AP, Ropelle ER, Røslund GV, Rossignol R, Rossiter HB,
 54 Rubelj I, Rybacka-Mossakowska J, Saada A, Safaei Z, Salin K, Salvadego D, Sandi C, Sanz A,
 55 Sazanov LA, Scatena R, Schartner M, Scheibye-Knudsen M, Schilling JM, Schlattner U, Schönfeld P,
 56 Schots P, Schulz R, Schwarzer C, Scott GR, Shabalina IG, Sharma P, Sharma V, Shevchuk I, Siewiera
 57 K, Silber AM, Silva AM, Sims CA, Singer D, Skolik R, Smenes BT, Smith J, Soares FAA, Sobotka
 58 O, Sokolova I, Sonkar VK, Sowton AP, Sparagna GC, Sparks LM, Spinazzi M, Stankova P, Starr J,
 59 Stary C, Stelfa G, Stiban J, Stier A, Stocker R, Storder J, Sumbalova Z, Suravajhala P, Svalbe B,
 60 Swerdlow RH, Swiniuch D, Szabo I, Szweczyk A, Szibor M, Tanaka M, Tandler B, Tarnopolsky MA,
 61 Tausan D, Tavernarakis N, Tepp K, Thakkar H, Thyfault JP, Tomar D, Torp MK, Towheed A, Tretter
 62 L, Trifunovic A, Trivigno C, Tronstad KJ, Trougakos IP, Truu L, Tuncay E, Turan B, Tyrrell DJ,
 63 Urban T, Valentine JM, Vella J, Vendelin M, Vercesi AE, Victor VM, Vieira Ligo Teixeira C, Viel C,
 64 Vieyra A, Vilks K, Villena JA, Vincent V, Vinogradov AD, Viscomi C, Vitorino RMP, Vogt S,
 65 Volani C, Volska K, Votion DM, Vujacic-Mirski K, Wagner BA, Ward ML, Warnsmann V,
 66 Wasserman DH, Watala C, Wei YH, Wickert A, Wieckowski MR, Wiesner RJ, Williams C,
 67 Winwood-Smith H, Wohlgemuth SE, Wohlwend M, Wolff J, Wüst RCI, Yokota T, Zablocki K,
 68 Zaugg K, Zaugg M, Zdrzilova L, Zhang Y, Zhang YZ, Zíková A, Zischka H, Zorzano A, Zvejniece L

69

70

Updates and discussion:

71

http://www.mitoeagle.org/index.php/MitoEAGLE_preprint_2018-02-08

72

73

Correspondence: Gnaiger E

74

Chair COST Action CA15203 MitoEAGLE – <http://www.mitoeagle.org>

75

Department of Visceral, Transplant and Thoracic Surgery, D. Swarovski Research Laboratory,

76

Medical University of Innsbruck, Innrain 66/4, A-6020 Innsbruck, Austria

77

Email: mitoeagle@i-med.ac.at; Tel: +43 512 566796, Fax: +43 512 566796 20

78



79	Table of contents
80	
81	Abstract
82	Executive summary
83	1. Introduction – Box 1: In brief: Mitochondria and Bioblasts
84	2. Coupling states and rates in mitochondrial preparations
85	2.1. <i>Cellular and mitochondrial respiration</i>
86	2.1.1. Aerobic and anaerobic catabolism and ATP turnover
87	2.1.2. Specification of biochemical dose
88	2.2. <i>Mitochondrial preparations</i>
89	2.3. <i>Electron transfer pathways</i>
90	2.4. <i>Respiratory coupling control</i>
91	2.4.1. Coupling
92	2.4.2. Phosphorylation, P _s , and P _s /O ₂ ratio
93	2.4.3. Uncoupling
94	2.5. <i>Coupling states and respiratory rates</i>
95	2.5.1. LEAK-state
96	2.5.2. OXPHOS-state
97	2.5.3. Electron transfer-state
98	2.5.4. ROX state and <i>Rox</i>
99	2.5.5. Quantitative relations
100	2.5.6. The steady-state
101	2.6. <i>Classical terminology for isolated mitochondria</i>
102	2.6.1. State 1
103	2.6.2. State 2
104	2.6.3. State 3
105	2.6.4. State 4
106	2.6.5. State 5
107	2.7. <i>Control and regulation</i>
108	3. What is a rate? – Box 2: Metabolic flows and fluxes: vectorial, vectorial, and scalar
109	4. Normalization of rate per sample
110	4.1. <i>Flow: per object</i>
111	4.1.1. Number concentration
112	4.1.2. Flow per object
113	4.2. <i>Size-specific flux: per sample size</i>
114	4.2.1. Sample concentration
115	4.2.2. Size-specific flux
116	4.3. <i>Marker-specific flux: per mitochondrial content</i>
117	4.3.1. Mitochondrial concentration and mitochondrial markers
118	4.3.2. mt-Marker-specific flux
119	5. Normalization of rate per system
120	5.1. <i>Flow: per chamber</i>
121	5.2. <i>Flux: per chamber volume</i>
122	5.2.1. System-specific flux
123	5.2.2. Advancement per volume
124	6. Conversion of units
125	7. Conclusions – Box 3: Recommendations for studies with mitochondrial preparations
126	References
127	Supplement
128	S1. Manuscript phases and versions - an open-access approach
129	S2. Authors
130	S3. Joining COST Actions
131	

132 **Abstract** As the knowledge base and importance of mitochondrial physiology to human health expands,
 133 the necessity for harmonizing the terminology concerning mitochondrial respiratory states and rates has
 134 become increasingly apparent. The chemiosmotic theory establishes the mechanism of energy
 135 transformation and coupling in oxidative phosphorylation. The unifying concept of the protonmotive
 136 force provides the framework for developing a consistent theoretical foundation of mitochondrial
 137 physiology and bioenergetics. We follow IUPAC guidelines on terminology in physical chemistry,
 138 extended by considerations on open systems and thermodynamics of irreversible processes. The
 139 concept-driven constructive terminology incorporates the meaning of each quantity and aligns concepts
 140 and symbols to the nomenclature of classical bioenergetics. We endeavour to provide a balanced view
 141 on mitochondrial respiratory control and a critical discussion on reporting data of mitochondrial
 142 respiration in terms of metabolic flows and fluxes. Uniform standards for evaluation of respiratory states
 143 and rates will ultimately contribute to reproducibility between laboratories and thus support the
 144 development of databases of mitochondrial respiratory function in species, tissues, and cells. Clarity of
 145 concept and consistency of nomenclature facilitate effective transdisciplinary communication,
 146 education, and ultimately further discovery.

147
 148 *Keywords:* Mitochondrial respiratory control, coupling control, mitochondrial preparations,
 149 protonmotive force, uncoupling, oxidative phosphorylation, OXPHOS, efficiency, electron transfer, ET;
 150 electron transfer system, ETS; proton leak, LEAK, residual oxygen consumption, ROX, State 2, State
 151 3, State 4, normalization, flow, flux, O₂
 152

153 **Executive summary**

154
 155 In view of the broad implications for health care, mitochondrial researchers face an increasing
 156 responsibility to disseminate their fundamental knowledge and novel discoveries to a wide range of
 157 stakeholders and scientists beyond the group of specialists. This requires implementation of a commonly
 158 accepted terminology within the discipline and standardization in the translational context. Authors,
 159 reviewers, journal editors, and lecturers are challenged to collaborate with the aim to harmonize the
 160 nomenclature in the growing field of mitochondrial physiology and bioenergetics, from evolutionary
 161 biology and comparative physiology to mitochondrial medicine. In the present communication we focus
 162 on the following concepts in mitochondrial physiology:

- 163 1. Aerobic respiration depends on the coupling of phosphorylation (ADP → ATP) to O₂ flux in
 164 catabolic reactions. Coupling in oxidative phosphorylation is mediated by the translocation of
 165 protons across the inner mitochondrial membrane through proton pumps generating or
 166 utilizing the protonmotive force, that is maintained between the mitochondrial matrix and
 167 intermembrane compartment or outer mitochondrial space. Compartmental coupling
 168 distinguishes this vectorial component of oxidative phosphorylation from glycolytic
 169 fermentation as the counterpart of cellular core energy metabolism (**Figure 1**). Cell respiration
 170 is distinguished from fermentation: (1) Electron acceptors are supplied by external respiration
 171 for the maintenance of redox balance, whereas fermentation is characterized by an internal
 172 electron acceptor produced in intermediary metabolism. In aerobic cell respiration, redox
 173 balance is maintained by O₂ as the electron acceptor. (2) Compartmental coupling in vectorial
 174 oxidative phosphorylation contrasts to exclusively scalar substrate-level phosphorylation in
 175 fermentation.
- 176 2. When measuring mitochondrial metabolism, the contribution of fermentation and other cytosolic
 177 interactions must be excluded from analysis by disrupting the barrier function of the plasma
 178 membrane. Selective removal or permeabilization of the plasma membrane yields
 179 mitochondrial preparations—including isolated mitochondria, tissue and cellular
 180 preparations—with structural and functional integrity. Subsequently, extra-mitochondrial
 181 concentrations of fuel substrates, ADP, ATP, inorganic phosphate, and cations including H⁺
 182 can be controlled to determine mitochondrial function under a set of conditions defined as
 183 *coupling control states*. We strive to incorporate an easily recognized and understood, concept-
 184 driven terminology of bioenergetics with explicit terms and symbols that define the nature of
 185 respiratory states.
- 186 3. Mitochondrial coupling states are defined according to the control of respiratory oxygen flux by
 187 the protonmotive force. Capacities of oxidative phosphorylation and electron transfer are

measured at kinetically saturating concentrations of fuel substrates, ADP and inorganic phosphate, and O₂, or at optimal uncoupler concentrations, respectively, in the absence of Complex IV inhibitors such as NO, CO, or H₂S. Respiratory capacity is a measure of the upper bound of the rate of respiration; it depends on the substrate type undergoing oxidation, and provides reference values for the diagnosis of health and disease, and for evaluation of the effects of Evolutionary background, Age, Gender and sex, Lifestyle and Environment.

Figure 1. Internal and external respiration

Mitochondrial respiration is the oxidation of fuel substrates (electron donors) and reduction of O₂ catalysed by the electron transfer system, ETS: (mt) mitochondrial catabolic respiration; (ce) total cellular O₂ consumption; and (ext) external respiration. All chemical reactions, r , that consume O₂ in the cells of an organism, contribute to cell respiration, J_{rO_2} . In addition to mitochondrial catabolic respiration, O₂ is consumed by:

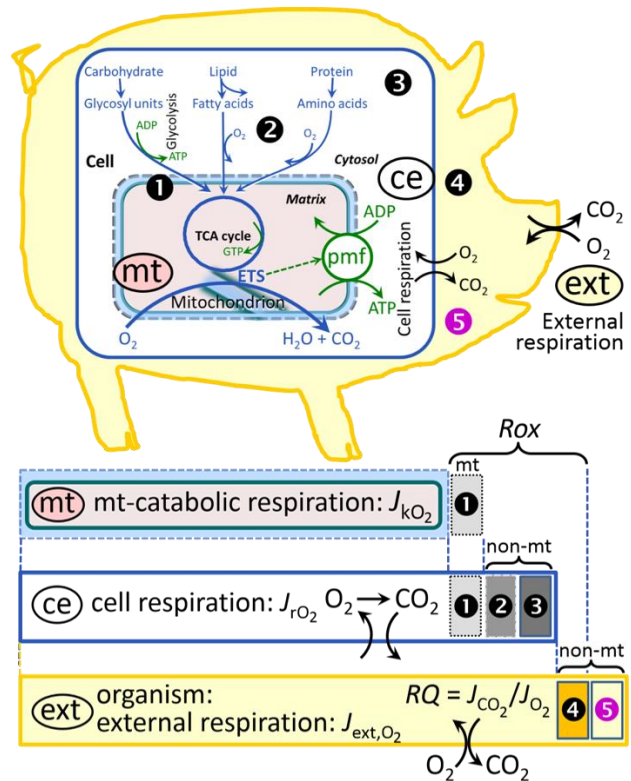
① Mitochondrial residual O₂ consumption, Rox .
 ② Non-mitochondrial O₂ consumption by catabolic reactions, particularly peroxisomal oxidases and microsomal cytochrome P450 systems. ③ Non-mitochondrial Rox by reactions unrelated to catabolism. ④ Extracellular Rox . ⑤ Aerobic microbial respiration. Bars are not at a quantitative scale.

(mt) **Mitochondrial catabolic respiration**, J_{kO_2} , is the O₂ consumption by the mitochondrial ETS excluding Rox .

(ce) **Cell respiration**, J_{rO_2} , takes into account

internal O₂-consuming reactions, r , including catabolic respiration and Rox . Catabolic cell respiration is the O₂ consumption associated with catabolic pathways in the cell, including mitochondrial catabolism in addition to peroxisomal and microsomal oxidation reactions (②).

(ext) **External respiration** balances internal respiration at steady-state, including extracellular Rox (④) and aerobic respiration by the microbiome (⑤). O₂ is transported from the environment across the respiratory cascade, *i.e.*, circulation between tissues and diffusion across cell membranes, to the intracellular compartment. The respiratory quotient, RQ , is the molar CO₂/O₂ exchange ratio; when combined with the respiratory nitrogen quotient, N/O₂ (mol N given off per mol O₂ consumed), the RQ reflects the proportion of carbohydrate, lipid and protein utilized in cell respiration during aerobically balanced steady-states. Bicarbonate and CO₂ are transported in reverse to the extracellular milieu and the organismic environment. Hemoglobin provides the molecular paradigm for the combination of O₂ and CO₂ exchange, as do lungs and gills on the morphological level.



4. Incomplete tightness of coupling, *i.e.*, some degree of uncoupling relative to the substrate-dependent coupling stoichiometry, is a characteristic of energy-transformations across membranes. Uncoupling is caused by a variety of physiological, pathological, toxicological, pharmacological and environmental conditions that exert an influence not only on the proton leak and cation cycling, but also on proton slip within the proton pumps and the structural integrity of the mitochondria. A more loosely coupled state is induced by stimulation of mitochondrial superoxide formation and the bypass of proton pumps. In addition, the use of protonophores represents an experimental uncoupling intervention to assess the transition from a well-coupled to a noncoupled state of mitochondrial respiration.

5. Respiratory oxygen consumption rates have to be carefully normalized to enable meta-analytic studies beyond the question of a particular experiment. Therefore, all raw data on rates and variables for normalization should be published in an open access data repository. Normalization of rates for: (1) the number of objects (cells, organisms); (2) the volume or

244 mass of the experimental sample; and (3) the concentration of mitochondrial markers in the
 245 experimental chamber are sample-specific normalizations, which are distinguished from
 246 system-specific normalization for the volume of the chamber (the measuring system).
 247 6. The consistent use of terms and symbols will facilitate transdisciplinary communication and
 248 support the further development of a collaborative database on bioenergetics and
 249 mitochondrial physiology. The present considerations are focused on studies with
 250 mitochondrial preparations. These will be extended in a series of reports on pathway control
 251 of mitochondrial respiration, respiratory states in intact cells, and harmonization of
 252 experimental procedures.
 253

254 **Box 1: In brief – Mitochondria and Bioblasts**

255 *‘For the physiologist, mitochondria afforded the first opportunity for an experimental*
 256 *approach to structure-function relationships, in particular those involved in active*
 257 *transport, vectorial metabolism, and metabolic control mechanisms on a subcellular level’*
 258 (Ernster and Schatz 1981).

259 Mitochondria are oxygen-consuming electrochemical generators that evolved from the endosymbiotic
 260 alphaproteobacteria which integrated into a host cell related to Asgard Archaea (Margulis 1970; Lane
 261 2005; Roger *et al.* 2017). They were described by Richard Altmann (1894) as ‘bioblasts’, which include
 262 not only the mitochondria as presently defined, but also symbiotic and free-living bacteria. The word
 263 ‘mitochondria’ (Greek mitos: thread; chondros: granule) was introduced by Carl Benda (1898).

264 Contrary to current textbook dogma, mitochondria form dynamic networks within eukaryotic
 265 cells. Mitochondrial movement is supported by microtubules and morphology can change in response
 266 to energy requirements of the cell via processes known as fusion and fission; these interactions allow
 267 mitochondria to communicate within a network (Chan 2006). Mitochondria can even traverse cell
 268 boundaries in a process known as horizontal mitochondrial transfer (Torralba *et al.* 2016). Another
 269 defining characteristic of mitochondria is the double membrane. The mitochondrial inner membrane
 270 (mtIM) forms dynamic tubular to disk-shaped cristae that separate the mitochondrial matrix, *i.e.*, the
 271 negatively charged internal mitochondrial compartment, from the intermembrane space; the latter being
 272 enclosed by the mitochondrial outer membrane (mtOM) and positively charged with respect to the
 273 matrix. The mtIM contains the non-bilayer phospholipid cardiolipin, which is not present in any other
 274 eukaryotic cellular membrane. Cardiolipin has many regulatory functions (Oemer *et al.* 2018); in
 275 particular, it stabilizes and promotes the formation of respiratory supercomplexes (SC I_nIII_nIV_n), which
 276 are supramolecular assemblies based upon specific and dynamic interactions between individual
 277 respiratory complexes (Greggio *et al.* 2017; Lenaz *et al.* 2017). The fluidity of the mitochondrial
 278 membrane is plastic and exerts an influence on the functional properties of proteins incorporated in
 279 membranes (Waczulikova *et al.* 2007). Intracellular stress factors may cause shrinking or swelling of
 280 the mitochondrial matrix, that can ultimately result in permeability transition.

281 Mitochondria are the structural and functional elementary components of cell respiration.
 282 Mitochondrial respiration is the reduction of molecular oxygen by electron transfer coupled to
 283 electrochemical proton translocation across the mtIM. In the process of oxidative phosphorylation
 284 (OXPHOS), the catabolic reaction of oxygen consumption is electrochemically coupled to the
 285 transformation of energy in the form of adenosine triphosphate (ATP; Mitchell 1961, 2011).
 286 Mitochondria are the powerhouses of the cell which contain the machinery of the OXPHOS-pathways,
 287 including transmembrane respiratory complexes (proton pumps with FMN, Fe-S and cytochrome *b*, *c*,
 288 *aa*₃ redox systems); alternative dehydrogenases and oxidases; the coenzyme ubiquinone (Q); F-ATPase
 289 or ATP synthase; the enzymes of the tricarboxylic acid cycle (TCA), fatty acid and amino acid oxidation;
 290 transporters of ions, metabolites and co-factors; iron/sulphur cluster synthesis; and mitochondrial
 291 kinases related to catabolic pathways. The mitochondrial proteome comprises over 1,200 proteins
 292 (Calvo *et al.* 2015; 2017), mostly encoded by nuclear DNA (nDNA), with a variety of functions, many
 293 of which are relatively well known (*e.g.*, proteins regulating mitochondrial biogenesis or apoptosis),
 294 while others are still under investigation, or need to be identified (*e.g.*, permeability transition pore,
 295 alanine transporter). Only recently has it been possible to use the mammalian mitochondrial proteome
 296 to discover and characterize the genetic basis of mitochondrial diseases (Williams *et al.* 2016; Palmfeldt
 297 and Bross 2017).

298 Numerous cellular processes are orchestrated by a constant crosstalk between mitochondria and
 299 other cellular components. For example, the crosstalk between mitochondria and the endoplasmic

300 reticulum is involved in the regulation of calcium homeostasis, cell division, autophagy, differentiation,
301 and anti-viral signaling (Murley and Nunnari 2016). Mitochondria contribute to the formation of
302 peroxisomes, which are hybrids of mitochondrial and ER-derived precursors (Sugiura *et al.* 2017).
303 Cellular mitochondrial homeostasis (mitostasis) is maintained through regulation at transcriptional,
304 post-translational and epigenetic levels. Cell signalling modules contribute to homeostatic regulation
305 throughout the cell cycle or even cell death by activating proteostatic modules (*e.g.*, the ubiquitin-
306 proteasome and autophagy-lysosome/vacuole pathways; specific proteases like LON) and genome
307 stability modules in response to varying energy demands and stress cues (Quiros *et al.* 2016). Several
308 post-translational modifications, including acetylation and nitrosylation, are also capable of influencing
309 the bioenergetic response, with clinically significant implications for health and disease (Carrico *et al.*
310 2018).

311 Mitochondria of higher eukaryotes typically maintain several copies of their own circular genome
312 known as mitochondrial DNA (mtDNA; hundred to thousands per cell; Cummins 1998), which is
313 maternally inherited in humans. Biparental mitochondrial inheritance is documented in mammals, birds,
314 fish, reptiles and invertebrate groups, and is even the norm in some bivalve taxonomic groups (Breton
315 *et al.* 2007; White *et al.* 2008). The mitochondrial genome of the angiosperm *Amborella* contains a
316 record of six mitochondrial genome equivalents acquired by horizontal transfer of entire genomes, two
317 from angiosperms, three from algae and one from mosses (Rice *et al.* 2016). In unicellular organisms
318 (*i.e.*, protists) the structural organization of mitochondrial genomes is highly variable and includes
319 circular and linear DNA (Zikova *et al.* 2016). While some of the free-living flagellates exhibit the largest
320 known gene coding capacity (*e.g.* jakobid *Andalucia godoyi* mitochondrial DNA codes for 106 genes;
321 Burger *et al.* 2013), some protist groups (*e.g.* alveolates) possess mitochondrial genomes with only three
322 protein-coding genes and two rRNAs (Feagin *et al.* 2012). The complete loss of mitochondrial genome
323 is observed in highly reduced mitochondria of *Cryptosporidium* species (Liu *et al.* 2016). Reaching the
324 final extreme, the microbial eukaryote, oxymonad *Monocercomonoides*, has no mitochondrion
325 whatsoever and lacks all typical nuclear-encoded mitochondrial proteins demonstrating that while in
326 99% of organisms mitochondria play a vital role, this organelle is not indispensable (Karnkowska *et al.*
327 2016).

328 In vertebrates but not all invertebrates, mtDNA is compact (16.5 kB in humans) and encodes 13
329 protein subunits of the transmembrane respiratory Complexes CI, CIII, CIV and ATP synthase (F-
330 ATPase), 22 tRNAs, and two rRNAs. Additional gene content has been suggested to include microRNAs,
331 piRNA, smithRNAs, repeat associated RNA, and even additional proteins (Duarte *et al.* 2014; Lee *et al.*
332 2015; Cobb *et al.* 2016). The mitochondrial genome requires nuclear-encoded mitochondrially
333 targeted proteins, *e.g.*, TFAM, for its maintenance and expression (Rackham *et al.* 2012). Both genomes
334 encode peptides of the membrane spanning redox pumps (CI, CIII and CIV) and F-ATPase, leading to
335 strong constraints in the coevolution of both genomes (Blier *et al.* 2001).

336 Given the multiple roles of mitochondria, it is perhaps not surprising that mitochondrial
337 dysfunction is associated with a wide variety of genetic and degenerative diseases. Robust mitochondrial
338 function is supported by physical exercise and caloric balance, and is central for sustained metabolic
339 health throughout life. Therefore, a more consistent set of definitions for mitochondrial physiology will
340 increase our understanding of the etiology of disease and improve the diagnostic repertoire of
341 mitochondrial medicine with a focus on protective medicine, lifestyle and healthy aging.

342 Mitochondrion is singular and mitochondria is plural. Abbreviation: mt, as generally used in
343 mtDNA.

344

345

346

347 1. Introduction

348

349 Mitochondria are the powerhouses of the cell with numerous physiological, molecular, and
350 genetic functions (**Box 1**). Every study of mitochondrial health and disease faces **Evolution, Age,**
351 **Gender and sex, Lifestyle, and Environment (MitoEAGLE)** as essential background conditions intrinsic
352 to the individual person or cohort, species, tissue and to some extent even cell line. As a large and
353 coordinated group of laboratories and researchers, the mission of the global MitoEAGLE Network is to
354 generate the necessary scale, type, and quality of consistent data sets and conditions to address this
355 intrinsic complexity. Harmonization of experimental protocols and implementation of a quality control

356 and data management system are required to interrelate results gathered across a spectrum of studies
357 and to generate a rigorously monitored database focused on mitochondrial respiratory function. In this
358 way, researchers from a variety of disciplines can compare their findings using clearly defined and
359 accepted international standards.

360 With an emphasis on quality of research, published data can be useful far beyond the specific
361 question of a particular experiment. For example, collaborative data sets support the development of
362 open-access databases such as those for National Institutes of Health sponsored research in genetics,
363 proteomics, and metabolomics. Indeed, enabling meta-analysis is the most economic way of providing
364 robust answers to biological questions (Cooper *et al.* 2009). However, the reproducibility of quantitative
365 results and databases depend on accurate measurements under strictly-defined conditions. Likewise,
366 meaningful interpretation and comparability of experimental outcomes requires standardisation of
367 protocols between research groups at different institutes. In addition to quality control, a conceptual
368 framework is also required to standardise and homogenise terminology and methodology. Vague or
369 ambiguous jargon can lead to confusion and may relegate valuable signals to wasteful noise. For this
370 reason, measured values must be expressed in standard units for each parameter used to define
371 mitochondrial respiratory function. A consensus on fundamental nomenclature and conceptual
372 coherence, however, are missing in the expanding field of mitochondrial physiology. To fill this gap,
373 the present communication provides an in-depth review on harmonization of nomenclature and
374 definition of technical terms, which are essential to improve the awareness of the intricate meaning of
375 current and past scientific vocabulary. This is important for documentation and integration into
376 databases in general, and quantitative modelling in particular (Beard 2005).

377 In this review, we focus on coupling states and fluxes through metabolic pathways of aerobic
378 energy transformation in mitochondrial preparations as a first step in the attempt to generate a
379 conceptually-oriented nomenclature in bioenergetics and mitochondrial physiology. Respiratory control
380 by fuel substrates and specific inhibitors of respiratory enzymes, coupling states of intact cells, and
381 respiratory flux control ratios will be reviewed in subsequent communications, prepared in the frame of
382 COST Action MitoEAGLE open to global bottom-up input.

383
384

385 **2. Coupling states and rates in mitochondrial preparations**

386 *‘Every professional group develops its own technical jargon for talking about matters of critical*
387 *concern ... People who know a word can share that idea with other members of their group, and*
388 *a shared vocabulary is part of the glue that holds people together and allows them to create a*
389 *shared culture’* (Miller 1991).

390

391 *2.1. Cellular and mitochondrial respiration*

392

393 **2.1.1. Aerobic and anaerobic catabolism and ATP turnover:** In respiration, electron transfer
394 is coupled to the phosphorylation of ADP to ATP, with energy transformation mediated by the
395 protonmotive force, pmf (**Figure 2**). Anabolic reactions are coupled to catabolism, both by ATP as the
396 intermediary energy currency and by small organic precursor molecules as building blocks for
397 biosynthesis. Glycolysis involves substrate-level phosphorylation of ADP to ATP in fermentation
398 without utilization of O₂, studied mainly in intact cells and organisms. Many cellular fuel substrates are
399 catabolized to acetyl-CoA or to glutamate, and further electron transfer reduces nicotinamide adenine
400 dinucleotide to NADH or flavin adenine dinucleotide to FADH₂. Subsequent mitochondrial electron
401 transfer to O₂ is coupled to proton translocation for the control of the protonmotive force and
402 phosphorylation of ADP (**Figure 2B and 2C**). In contrast, extra-mitochondrial oxidation of fatty acids
403 and amino acids proceeds partially in peroxisomes without coupling to ATP production: acyl-CoA
404 oxidase catalyzes the oxidation of FADH₂ with electron transfer to O₂; amino acid oxidases oxidize
405 flavin mononucleotide FMNH₂ or FADH₂ (**Figure 2A**).

406

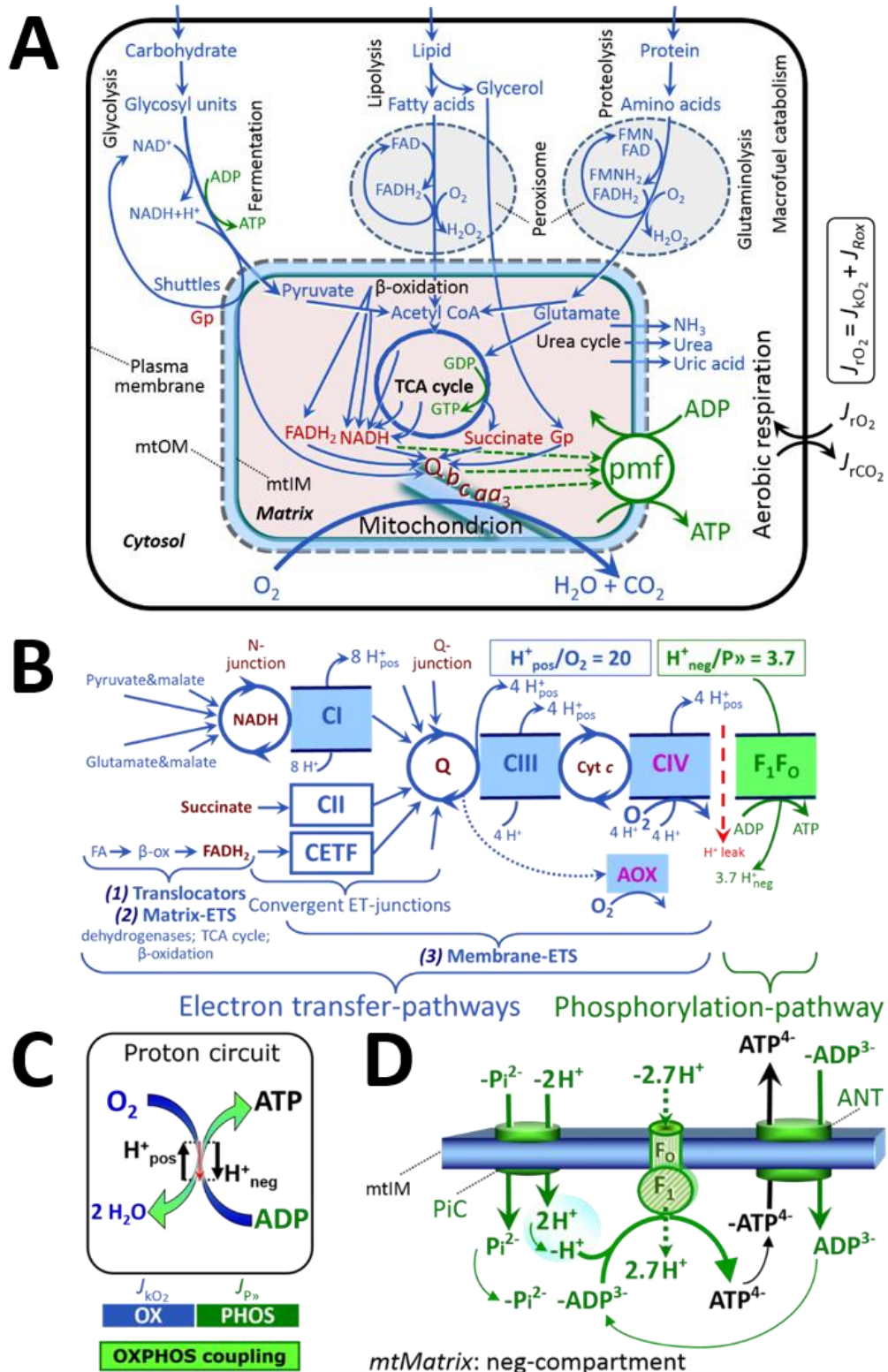


Figure 2. Cell respiration and oxidative phosphorylation (OXPHOS)

Mitochondrial respiration is the oxidation of fuel substrates (electron donors) with electron transfer to O_2 as the electron acceptor. For explanation of symbols see also **Figure 1**.

(A) Respiration of intact cells: Extra-mitochondrial catabolism of macrofuels and uptake of small molecules by the cell provide the mitochondrial fuel substrates. Dashed arrows indicate the connection between the redox proton pumps (respiratory Complexes CI, CIII and CIV) and the transmembrane protonmotive force, pmf. Coenzyme Q (Q) and the cytochromes *b*, *c*, and *aa₃* are redox systems of the mitochondrial inner membrane, mtIM. Glycerol-3-phosphate, Gp.

407
408
409
410
411
412
413
414
415
416

417 (B) Respiration in mitochondrial preparations: The mitochondrial electron transfer system
 418 (ETS) is (1) fuelled by diffusion and transport of substrates across the mtOM and mtIM,
 419 and in addition consists of the (2) matrix-ETS, and (3) membrane-ETS. Electron transfer
 420 converges at the N-junction, and from CI, CII and electron transferring flavoprotein
 421 complex (CETF) at the Q-junction. Unspecified arrows converging at the Q-junction
 422 indicate additional ETS-sections with electron entry into Q through glycerophosphate
 423 dehydrogenase, dihydro-orotate dehydrogenase, proline dehydrogenase, choline
 424 dehydrogenase, and sulfide-ubiquinone oxidoreductase. The dotted arrow indicates the
 425 branched pathway of oxygen consumption by alternative quinol oxidase (AOX). ET-
 426 pathways are coupled to the phosphorylation-pathway. The H^+_{pos}/O_2 ratio is the outward
 427 proton flux from the matrix space to the positively (pos) charged vesicular compartment,
 428 divided by catabolic O_2 flux in the NADH-pathway. The $H^+_{\text{neg}}/P_{\text{P}}$ ratio is the inward proton
 429 flux from the inter-membrane space to the negatively (neg) charged matrix space, divided
 430 by the flux of phosphorylation of ADP to ATP. These stoichiometries are not fixed due to
 431 ion leaks and proton slip. Modified from Lemieux *et al.* (2017) and Rich (2013).
 432 (C) OXPHOS coupling: O_2 flux through the catabolic ET-pathway, J_{kO_2} , is coupled
 433 by the H^+ circuit to flux through the phosphorylation-pathway of ADP to ATP, $J_{P_{\text{P}}}$.
 434 (D) Chemiosmotic phosphorylation-pathway catalyzed by the proton pump F_1F_0 -ATPase
 435 (F-ATPase, ATP synthase), adenine nucleotide translocase (ANT), and inorganic
 436 phosphate carrier (PiC). The $H^+_{\text{neg}}/P_{\text{P}}$ stoichiometry is the sum of the coupling
 437 stoichiometry in the F-ATPase reaction ($-2.7 H^+_{\text{pos}}$ from the positive intermembrane space,
 438 $2.7 H^+_{\text{neg}}$ to the matrix, *i.e.*, the negative compartment) and the proton balance in the
 439 translocation of ADP^{3-} , ATP^{4-} and P_i^{2-} . Modified from Gnaiger (2014).
 440

441 The plasma membrane separates the intracellular compartment including the cytosol, nucleus, and
 442 organelles from the extracellular environment. The plasma membrane consists of a lipid bilayer with
 443 embedded proteins and attached organic molecules that collectively control the selective permeability
 444 of ions, organic molecules, and particles across the cell boundary. The intact plasma membrane prevents
 445 the passage of many water-soluble mitochondrial substrates and inorganic ions—such as succinate,
 446 adenosine diphosphate (ADP) and inorganic phosphate (P_i), that must be precisely controlled at
 447 kinetically-saturating concentrations for the analysis of mitochondrial respiratory capacities.
 448 Respiratory capacities delineate, comparable to channel capacity in information theory (Schneider
 449 2006), the upper bound of the rate of O_2 consumption measured in defined respiratory states. Despite
 450 the activity of solute carriers, *e.g.*, SLC13A3 and SLC20A2, which transport specific metabolites across
 451 the plasma membrane of various cell types, the intact plasma membrane limits the scope of
 452 investigations into mitochondrial respiratory function in intact cells.

453 **2.1.2. Specification of biochemical dose:** Substrates, uncouplers, inhibitors, and other chemical
 454 reagents are titrated to analyse cellular and mitochondrial function. Nominal concentrations of these
 455 substances are usually reported as initial amount of substance concentration [$\text{mol}\cdot\text{L}^{-1}$] in the incubation
 456 medium. When aiming at the measurement of kinetically saturated processes—such as OXPHOS-
 457 capacities, the concentrations for substrates can be chosen according to the apparent equilibrium
 458 constant, K_m' . In the case of hyperbolic kinetics, only 80% of maximum respiratory capacity is obtained
 459 at a substrate concentration of four times the K_m' , whereas substrate concentrations of 5, 9, 19 and 49
 460 times the K_m' are theoretically required for reaching 83%, 90%, 95% or 98% of the maximal rate
 461 (Gnaiger 2001). Other reagents are chosen to inhibit or alter a particular process. The amount of these
 462 chemicals in an experimental incubation is selected to maximize effect, avoiding unacceptable off-target
 463 consequences that would adversely affect the data being sought. Specifying the amount of substance in
 464 an incubation as nominal concentration in the aqueous incubation medium can be ambiguous (Doskey
 465 *et al.* 2015), particularly for cations (TPP⁺; fluorescent dyes such as safranin, TMRM; Chowdhury *et al.*
 466 2015) and lipophilic substances (oligomycin, uncouplers, permeabilization agents; Doerrier *et al.* 2018),
 467 which accumulate in the mitochondrial matrix or in biological membranes, respectively. Generally,
 468 dose/exposure can be specified per unit of biological sample, *i.e.*, (nominal moles of
 469 xenobiotic)/(number of cells) [$\text{mol}\cdot\text{cell}^{-1}$] or, as appropriate, per mass of biological sample [$\text{mol}\cdot\text{kg}^{-1}$].
 470 This approach to specification of dose/exposure provides a scalable parameter that can be used to design
 471 experiments, help interpret a wide variety of experimental results, and provide absolute information that
 472 allows researchers worldwide to make the most use of published data (Doskey *et al.* 2015).

473 2.2. Mitochondrial preparations

474

475

476 Mitochondrial preparations are defined as either isolated mitochondria, or tissue and cellular
 477 preparations in which the barrier function of the plasma membrane is disrupted. Since this entails the
 478 loss of cell viability, mitochondrial preparations are not studied *in vivo*. In contrast to isolated
 479 mitochondria and tissue homogenate preparations, mitochondria in permeabilized tissues and cells are
 480 *in situ* relative to the plasma membrane. When studying mitochondrial preparations, substrate-
 481 uncoupler-inhibitor-titration (SUIT) protocols are used to establish respiratory coupling control states
 482 (CCS) and pathway control states (PCS) that provide reference values for various output variables
 483 (**Table 1**). Physiological conditions *in vivo* deviate from these experimentally obtained states; this is
 484 because kinetically-saturating concentrations, *e.g.*, of ADP, oxygen (O₂; dioxygen) or fuel substrates,
 485 may not apply to physiological intracellular conditions. Further information is obtained in studies of
 486 kinetic responses to variations in fuel substrate concentrations, [ADP], or [O₂] in the range between
 487 kinetically-saturating concentrations and anoxia (Gnaiger 2001).

488

489 The cholesterol content of the plasma membrane is high compared to mitochondrial membranes
 490 (Korn 1969). Therefore, mild detergents—such as digitonin and saponin—can be applied to selectively
 491 permeabilize the plasma membrane via interaction with cholesterol; this allows free exchange of organic
 492 molecules and inorganic ions between the cytosol and the immediate cell environment, while
 493 maintaining the integrity and localization of organelles, cytoskeleton, and the nucleus. Application of
 494 permeabilization agents (mild detergents or toxins) leads to washout of cytosolic marker enzymes—
 495 such as lactate dehydrogenase—and results in the complete loss of cell viability (tested by nuclear
 496 staining using plasma membrane-impermeable dyes), while mitochondrial function remains intact
 497 (tested by cytochrome *c* stimulation of respiration). Digitonin concentrations have to be optimized
 498 according to cell type, particularly since mitochondria from cancer cells contain significantly higher
 499 contents of cholesterol in both membranes (Baggetto and Testa-Perussini, 1990). For example, a dose
 500 of digitonin of 8 fmol·cell⁻¹ (10 pg·cell⁻¹; 10 μg·10⁻⁶ cells) is optimal for permeabilization of endothelial
 501 cells, and the concentration in the incubation medium has to be adjusted according to the cell density
 502 applied (Doerrier *et al.* 2018). Respiration of isolated mitochondria remains unaltered after the addition
 503 of low concentrations of digitonin or saponin. In addition to mechanical cell disruption during
 504 homogenization of tissue, permeabilization agents may be applied to ensure permeabilization of all cells
 505 in tissue homogenates.

506

507 Suspensions of cells permeabilized in the respiration chamber and crude tissue homogenates
 508 contain all components of the cell at highly dilute concentrations. All mitochondria are retained in
 509 chemically-permeabilized mitochondrial preparations and crude tissue homogenates. In the preparation
 510 of isolated mitochondria, however, the mitochondria are separated from other cell fractions and purified
 511 by differential centrifugation, entailing the loss of mitochondria at typical recoveries ranging from 30%
 512 to 80% of total mitochondrial content (Lai *et al.* 2018). Using Percoll or sucrose density gradients to
 513 maximize the purity of isolated mitochondria may compromise the mitochondrial yield or structural and
 514 functional integrity. Therefore, mitochondrial isolation protocols need to be optimized according to each
 515 study. The term mitochondrial preparation does neither include intact cells, nor submitochondrial
 516 particles and further fractionation of mitochondrial components.

517

518 2.3. Electron transfer pathways

519

520 Mitochondrial electron transfer (ET) pathways are fuelled by diffusion and transport of substrates
 521 across the mtOM and mtIM. In addition, the mitochondrial electron transfer system (ETS) consists of
 522 the matrix-ETS, and membrane-ETS (**Figure 2B**). Upstream sections of ET-pathways converge at the
 523 NADH-junction (N-junction). NADH is mainly generated in the tricarboxylic acid (TCA) cycle and is
 524 oxidized by Complex I (CI), with further electron entry into the coenzyme Q-junction (Q-junction).
 525 Similarly, succinate is formed in the TCA cycle and oxidized by CII to fumarate. CII is part of both the
 526 TCA cycle and the ETS, and reduces FAD to FADH₂ with further reduction of ubiquinone to ubiquinol
 527 downstream of the TCA cycle in the Q-junction. Thus FADH₂ is not a substrate but is the product of
 528 CII, in contrast to erroneous metabolic maps shown in many publications. β-oxidation of fatty acids
 (FA) generates FADH₂ as the substrate of electron transferring flavoprotein complex (ETF).

529

530 Selected mitochondrial catabolic pathways, *k*, of electron transfer from the oxidation of fuel
 531 substrates to the reduction of O₂ are activated by depletion of endogenous substrates and addition of fuel

532

529 substrates to the mitochondrial respiration medium (**Figure 2B**). Substrate combinations and specific
 530 inhibitors of ET-pathway enzymes are used to obtain defined pathway control states in mitochondrial
 531 preparations (Gnaiger 2014).

532

533 2.4. Respiratory coupling control

534

535 **2.4.1. Coupling:** In mitochondrial electron transfer, vectorial transmembrane proton flux is
 536 coupled through the redox proton pumps CI, CIII and CIV to the catabolic flux of scalar reactions,
 537 collectively measured as O₂ flux, J_{KO_2} (**Figure 2**). Thus mitochondria are elementary components of
 538 energy transformation. Energy is a conserved quantity and cannot be lost or produced in any internal
 539 process (First Law of thermodynamics). Open and closed systems can gain or lose energy only by
 540 external fluxes—by exchange with the environment. Therefore, energy can neither be produced by
 541 mitochondria, nor is there any internal process without energy conservation. Exergy or Gibbs energy
 542 ('free energy') is the part of energy that can potentially be transformed into work under conditions of
 543 constant temperature and pressure. *Coupling* is the interaction of an exergonic process (spontaneous,
 544 negative exergy change) with an endergonic process (positive exergy change) in energy transformations
 545 which conserve part of the exergy that would be irreversibly lost or dissipated in an uncoupled process.

546 Pathway control states (PCS) and coupling control states (CCS) are complementary, since
 547 mitochondrial preparations depend on (1) an exogenous supply of pathway-specific fuel substrates and
 548 oxygen, and (2) exogenous control of phosphorylation (**Figure 2**).

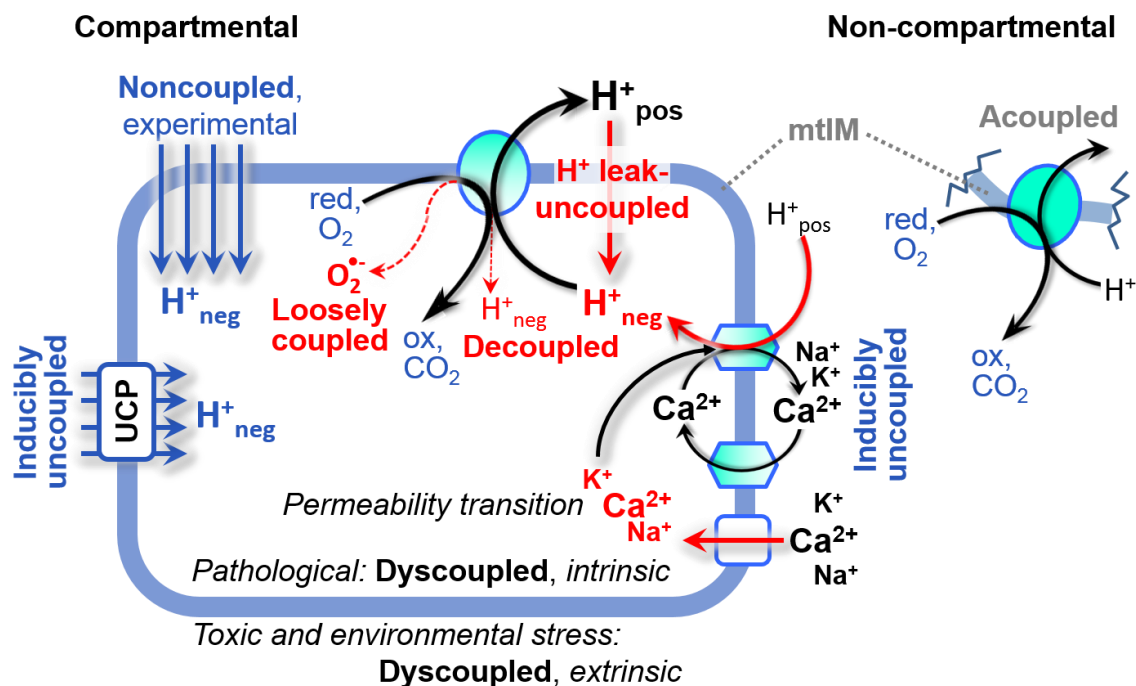
549 **2.4.2. Phosphorylation, P», and P»/O₂ ratio:** Phosphorylation in the context of OXPHOS is
 550 defined as phosphorylation of ADP by P_i to form ATP. On the other hand, the term phosphorylation is
 551 used generally in many contexts, *e.g.*, protein phosphorylation. This justifies consideration of a symbol
 552 more discriminating and specific than P as used in the P/O ratio (phosphate to atomic oxygen ratio),
 553 where P indicates phosphorylation of ADP to ATP or GDP to GTP (**Figure 2**). We propose the symbol
 554 P» for the endergonic (uphill) direction of phosphorylation ADP→ATP, and likewise the symbol P« for
 555 the corresponding exergonic (downhill) hydrolysis ATP→ADP. P» refers mainly to electrontransfer
 556 phosphorylation but may also involve substrate-level phosphorylation as part of the TCA cycle
 557 (succinyl-CoA ligase; phosphoglycerate kinase) and phosphorylation of ADP catalyzed by pyruvate
 558 kinase, and of GDP phosphorylated by phosphoenolpyruvate carboxykinase. Transphosphorylation is
 559 performed by adenylate kinase, creatine kinase (mtCK), hexokinase and nucleoside diphosphate kinase.
 560 In isolated mammalian mitochondria, ATP production catalyzed by adenylate kinase (2 ADP ↔ ATP +
 561 AMP) proceeds without fuel substrates in the presence of ADP (Komlódi and Tretter 2017). Kinase
 562 cycles are involved in intracellular energy transfer and signal transduction for regulation of energy flux.

563 The P»/O₂ ratio (P»/4 e⁻) is two times the 'P/O' ratio (P»/2 e⁻) of classical bioenergetics. P»/O₂ is
 564 a generalized symbol, not specific for determination of P_i consumption (P_i/O₂ flux ratio), ADP depletion
 565 (ADP/O₂ flux ratio), or ATP production (ATP/O₂ flux ratio). The mechanistic P»/O₂ ratio—or P»/O₂
 566 stoichiometry—is calculated from the proton-to-O₂ and proton-to-phosphorylation coupling
 567 stoichiometries (**Figure 2B**):

$$569 \quad \text{P}\gg/\text{O}_2 = \frac{H_{\text{pos}}^+/\text{O}_2}{H_{\text{neg}}^+/\text{P}\gg} \quad (1)$$

571 The H⁺_{pos}/O₂ coupling stoichiometry (referring to the full 4 electron reduction of O₂) depends on the
 572 relative involvement of the three coupling sites (respiratory Complexes CI, CIII and CIV) in the
 573 catabolic ET-pathway from reduced fuel substrates (electron donors) to the reduction of O₂ (electron
 574 acceptor). This varies with: (1) a bypass of CI by single or multiple electron input into the Q-junction;
 575 and (2) a bypass of CIV by involvement of alternative oxidases, AOX, which are not expressed in
 576 mammalian mitochondria.

577 The H⁺_{pos}/O₂ coupling stoichiometry equals 12 in the ET-pathways involving CIII and CIV as
 578 proton pumps, increasing to 20 for the NADH-pathway through CI (**Figure 2B**), but a general consensus
 579 on H⁺_{pos}/O₂ stoichiometries remains to be reached (Hinkle 2005; Wikström and Hummer 2012; Sazanov
 580 2015). The H⁺_{neg}/P» coupling stoichiometry (3.7; **Figure 2B**) is the sum of 2.7 H⁺_{neg} required by the F-
 581 ATPase of vertebrate and most invertebrate species (Watt *et al.* 2010) and the proton balance in the
 582 translocation of ADP, ATP and P_i (**Figure 2C**). Taken together, the mechanistic P»/O₂ ratio is calculated
 583 at 5.4 and 3.3 for NADH- and succinate-linked respiration, respectively (Eq. 1). The corresponding
 584 classical P»/O ratios (referring to the 2 electron reduction of 0.5 O₂) are 2.7 and 1.6 (Watt *et al.* 2010),
 585 in agreement with the measured P»/O ratio for succinate of 1.58 ± 0.02 (Gnaiger *et al.* 2000).



587
588
589
590
591
592
593
594
595
596
597
598
599

Figure 3. Mechanisms of respiratory uncoupling

An intact mitochondrial inner membrane, mtIM, is required for vectorial, compartmental coupling. ‘Acoupled’ respiration is the consequence of structural disruption with catalytic activity of non-compartmental mitochondrial fragments. Inducible uncoupling (*e.g.*, by activation of UCP1) increases LEAK respiration; experimentally noncoupled respiration provides an estimate of ET-capacity obtained by titration of protonophores stimulating respiration to maximum O_2 flux. H^+ leak-uncoupled, decoupled, and loosely coupled respiration are components of intrinsic uncoupling (Table 2). Pathological dysfunction may affect all types of uncoupling, including permeability transition, causing intrinsically dyscoupled respiration. Similarly, toxicological and environmental stress factors can cause extrinsically dyscoupled respiration. Reduced fuel substrates, red; oxidized products, ox.

600 **2.4.3. Uncoupling:** The effective P_{\gg}/O_2 flux ratio ($Y_{P_{\gg}/O_2} = J_{P_{\gg}}/J_{KO_2}$) is diminished relative to the mechanistic P_{\gg}/O_2 ratio by intrinsic and extrinsic uncoupling or dyscoupling (Figure 3). Such generalized uncoupling is different from switching to mitochondrial pathways that involve fewer than three proton pumps (‘coupling sites’: Complexes CI, CIII and CIV), bypassing CI through multiple electron entries into the Q-junction, or CIII and CIV through AOX (Figure 2B). Reprogramming of mitochondrial pathways leading to different types of substrates being oxidized may be considered as a switch of gears (changing the stoichiometry by altering the substrate that is oxidized) rather than uncoupling (loosening the tightness of coupling relative to a fixed stoichiometry). In addition, Y_{P_{\gg}/O_2} depends on several experimental conditions of flux control, increasing as a hyperbolic function of [ADP] to a maximum value (Gnaiger 2001).

610 Uncoupling of mitochondrial respiration is a general term comprising diverse mechanisms:

- 611 1. Proton leak across the mtIM from the pos- to the neg-compartment (H^+ leak-uncoupled; Figure 612 3).
- 613 2. Cycling of other cations, strongly stimulated by permeability transition; comparable to the use of 614 protonophores, cation cycling is experimentally induced by valinomycin in the presence of K^+ ;
- 615 3. Decoupling by proton slip in the redox proton pumps when protons are effectively not pumped 616 (CI, CIII and CIV) or are not driving phosphorylation (F-ATPase);
- 617 4. Loss of vesicular (compartmental) integrity when electron transfer is acoupled;
- 618 5. Electron leak in the loosely coupled univalent reduction of O_2 to superoxide ($O_2^{\bullet -}$; superoxide 619 anion radical).

620 Differences of terms—uncoupled vs. noncoupled—are easily overlooked, although they relate to 621 different meanings of uncoupling (Figure 3 and Table 2).

622 2.5. Coupling states and respiratory rates

623

624

625

626

627

628

629

630

631

632

633

634

635

To extend the classical nomenclature on mitochondrial coupling states (Section 2.6) by a concept-driven terminology that explicitly incorporates information on the meaning of respiratory states, the terminology must be general and not restricted to any particular experimental protocol or mitochondrial preparation (Gnaiger 2009). Concept-driven nomenclature aims at mapping the meaning and concept behind the words and acronyms onto the forms of words and acronyms (Miller 1991). The focus of concept-driven nomenclature is primarily the conceptual *why*, along with clarification of the experimental *how*.

Table 1. Coupling states and residual oxygen consumption in mitochondrial preparations in relation to respiration- and phosphorylation-flux, J_{KO_2} and J_{P} , and protonmotive force, pmf. Coupling states are established at kinetically-saturating concentrations of fuel substrates and O_2 .

State	J_{KO_2}	J_{P}	pmf	Inducing factors	Limiting factors
LEAK	L ; low, cation leak-dependent respiration	0	max.	back-flux of cations including proton leak, proton slip	$J_{\text{P}} = 0$: (1) without ADP, L_{N} ; (2) max. ATP/ADP ratio, L_{T} ; or (3) inhibition of the phosphorylation-pathway, L_{Omy}
OXPHOS	P ; high, ADP-stimulated respiration, OXPHOS-capacity	max.	high	kinetically-saturating [ADP] and $[\text{P}_i]$	J_{P} by phosphorylation-pathway; or J_{KO_2} by ET-capacity
ET	E ; max., noncoupled respiration, ET-capacity	0	low	optimal external uncoupler concentration for max. $J_{\text{O}_2, \text{E}}$	J_{KO_2} by ET-capacity
ROX	R_{ox} ; min., residual O_2 consumption	0	0	$J_{\text{O}_2, \text{Rox}}$ in non-ET-pathway oxidation reactions	inhibition of all ET-pathways; or absence of fuel substrates

636

637

638

639

640

641

642

643

644

645

646

647

648

649

650

651

652

653

654

655

656

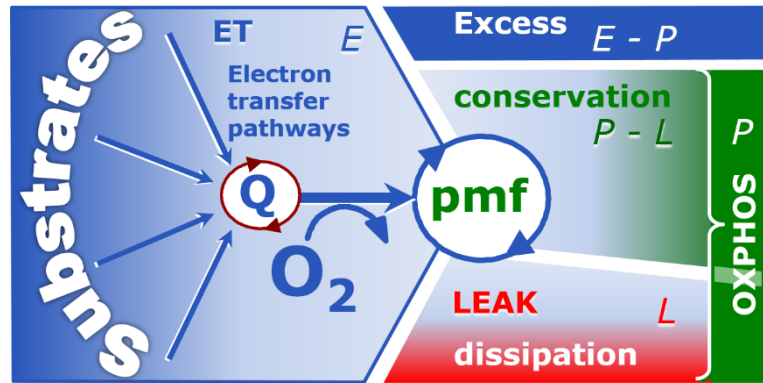
657

To provide a diagnostic reference for respiratory capacities of core energy metabolism, the capacity of oxidative phosphorylation, OXPHOS, is measured at kinetically-saturating concentrations of ADP and P_i . The oxidative ET-capacity reveals the limitation of OXPHOS-capacity mediated by the phosphorylation-pathway. The ET- and phosphorylation-pathways comprise coupled segments of the OXPHOS-system. ET-capacity is measured as noncoupled respiration by application of external uncouplers. The contribution of intrinsically uncoupled O_2 consumption is studied by preventing the stimulation of phosphorylation either in the absence of ADP or by inhibition of the phosphorylation-pathway. The corresponding states are collectively classified as LEAK-states, when O_2 consumption compensates mainly for ion leaks, including the proton leak. Defined coupling states are induced by: (1) adding cation chelators such as EGTA, binding free Ca^{2+} and thus limiting cation cycling; (2) adding ADP and P_i ; (3) inhibiting the phosphorylation-pathway; and (4) uncoupler titrations, while maintaining a defined ET-pathway state with constant fuel substrates and inhibitors of specific branches of the ET-pathway.

The three coupling states, ET, LEAK and OXPHOS, are shown schematically with the corresponding respiratory rates, abbreviated as E , L and P , respectively (**Figure 4**). We distinguish metabolic *pathways* from metabolic *states* and the corresponding metabolic *rates*; for example: ET-pathways, ET-states, and ET-capacities, E , respectively (**Table 1**). The protonmotive force is *high* in the OXPHOS-state when it drives phosphorylation, *maximum* in the LEAK-state of coupled mitochondria, driven by LEAK-respiration at a minimum back-flux of cations to the matrix side, and *very low* in the ET-state when uncouplers short-circuit the proton cycle (**Table 1**).

658 **Figure 4. Four-compartment**
 659 **model of oxidative**
 660 **phosphorylation**

661 Respiratory states (ET, OXPHOS,
 662 LEAK; Table 1) and corresponding
 663 rates (E , P , L) are connected by the
 664 protonmotive force, pmf. (1) ET-
 665 capacity, E , is partitioned into (2)
 666 dissipative LEAK-respiration, L ,
 667 when the Gibbs energy change of
 668 catabolic O_2 flux is irreversibly lost,
 669 (3) net OXPHOS-capacity, $P-L$, with
 670 partial conservation of the capacity to
 671 perform work, and (4) the excess capacity,
 $E-P$. Modified from Gnaiger (2014).

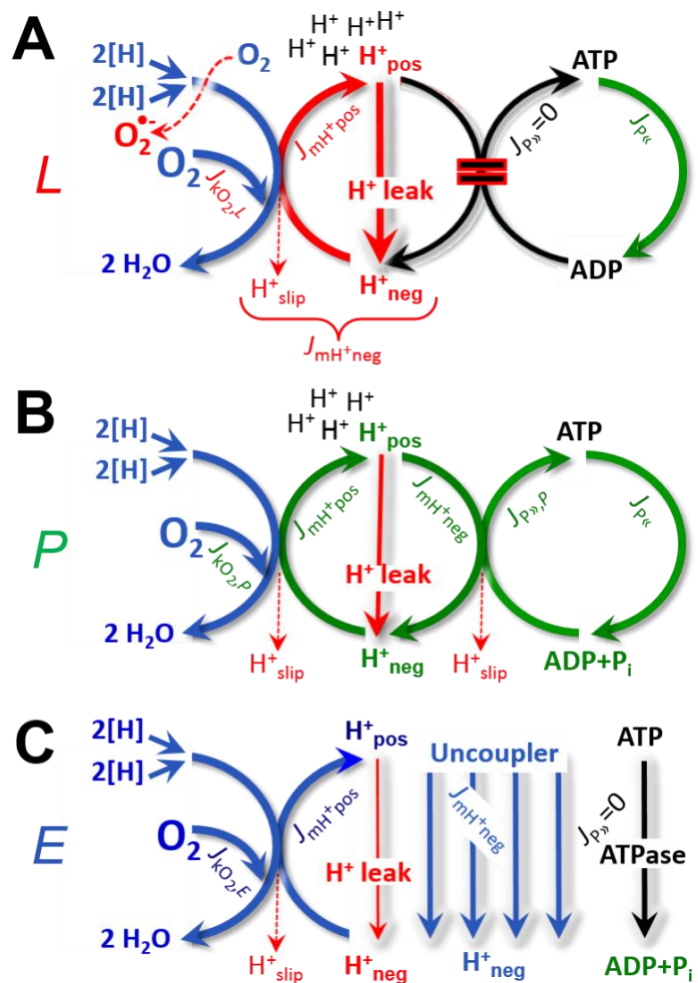


672 **Figure 5. Respiratory coupling**
 673 **states**

674 (A) **LEAK-state and rate, L** :
 675 Oxidation only, since phosphorylation
 676 is arrested, $J_{P\gg} = 0$, and catabolic O_2
 677 flux, $J_{kO_2,L}$, is controlled mainly by the
 678 proton leak and slip, J_{mH^+neg} , at
 679 maximum protonmotive force (Figure
 680 4). Extramitochondrial ATP may be
 681 hydrolyzed by extramitochondrial
 ATPases, $J_{P\ll}$; then phosphorylation
 must be blocked.

(B) **OXPHOS-state and rate, P** :
 Oxidation coupled to
 phosphorylation, $J_{P\gg}$, which is
 stimulated by kinetically-saturating
 [ADP] and $[P_i]$, supported by a high
 protonmotive force. O_2 flux, $J_{kO_2,P}$,
 is well-coupled at a $P\gg/O_2$ ratio of
 $J_{P\gg,P}/J_{O_2,P}$. Extramitochondrial
 ATPases may recycle ATP, $J_{P\ll}$.

(C) **ET-state and rate, E** : Oxidation
 only, since phosphorylation is zero,
 $J_{P\gg} = 0$, at optimum exogenous
 uncoupler concentration when
 noncoupled respiration, $J_{kO_2,E}$, is
 maximum. The F-ATPase may
 hydrolyze extramitochondrial ATP.



672

673

674 **2.5.1. LEAK-state (Figure 5A):** The LEAK-state is defined as a state of mitochondrial
 675 respiration when O_2 flux mainly compensates for ion leaks in the absence of ATP synthesis, at
 676 kinetically-saturating concentrations of O_2 , respiratory fuel substrates and P_i . LEAK-respiration is
 677 measured to obtain an estimate of intrinsic uncoupling without addition of an experimental uncoupler:
 678 (1) in the absence of adenylates, *i.e.*, AMP, ADP and ATP; (2) after depletion of ADP at a maximum
 679 ATP/ADP ratio; or (3) after inhibition of the phosphorylation-pathway by inhibitors of F-ATPase—such
 680 as oligomycin, or of adenine nucleotide translocase—such as carboxyatractylsido. Adjustment of the
 681 nominal concentration of these inhibitors to the density of biological sample applied can minimize or
 avoid inhibitory side-effects exerted on ET-capacity or even some dyscoupling.

682

Table 2. Terms on respiratory coupling and uncoupling.

Term	J_{kO_2}	$P \gg O_2$	Notes	
acoupled		0	electron transfer in mitochondrial fragments without vectorial proton translocation (Figure 3)	
intrinsic, no protonophore added	uncoupled	L	0	non-phosphorylating LEAK-respiration (Figure 5A)
	proton leak-uncoupled		0	component of L , H^+ diffusion across the mtIM (Figure 3)
	decoupled		0	component of L , proton slip (Figure 3)
	loosely coupled		0	component of L , lower coupling due to superoxide formation and bypass of proton pumps by electron leak (Figure 3)
	dyscoupled		0	pathologically, toxicologically, environmentally increased uncoupling, mitochondrial dysfunction
	inducibly uncoupled		0	by UCP1 or cation (<i>e.g.</i> , Ca^{2+}) cycling (Figure 3)
noncoupled	E	0	ET-capacity, non-phosphorylating respiration stimulated to maximum flux at optimum exogenous protonophore concentration (Figure 5C)	
well-coupled	P	high	OXPHOS-capacity , phosphorylating respiration with an intrinsic LEAK component (Figure 5B)	
fully coupled	$P - L$	max.	OXPHOS-capacity corrected for LEAK-respiration (Figure 4)	

683

684

685

686

687

688

689

690

691

692

693

694

695

696

697

698

699

700

701

702

703

704

705

706

707

708

709

710

- **Proton leak and uncoupled respiration:** The intrinsic proton leak is the *uncoupled* leak current of protons in which protons diffuse across the mtIM in the dissipative direction of the downhill protonmotive force without coupling to phosphorylation (**Figure 5A**). The proton leak flux depends non-linearly on the protonmotive force (Garlid *et al.* 1989; Divakaruni and Brand 2011), which is a temperature-dependent property of the mtIM and may be enhanced due to possible contaminations by free fatty acids. Inducible uncoupling mediated by uncoupling protein 1 (UCP1) is physiologically controlled, *e.g.*, in brown adipose tissue. UCP1 is a member of the mitochondrial carrier family that is involved in the translocation of protons across the mtIM (Klingenberg 2017). Consequently, this short-circuit lowers the protonmotive force and stimulates electron transfer, respiration, and heat dissipation in the absence of phosphorylation of ADP.
- **Cation cycling:** There can be other cation contributors to leak current including calcium and probably magnesium. Calcium influx is balanced by mitochondrial Na^+/Ca^{2+} or H^+/Ca^{2+} exchange, which is balanced by Na^+/H^+ or K^+/H^+ exchanges. This is another effective uncoupling mechanism different from proton leak (**Table 2**).
- **Proton slip and decoupled respiration:** Proton slip is the *decoupled* process in which protons are only partially translocated by a redox proton pump of the ET-pathways and slip back to the original vesicular compartment. The proton leak is the dominant contributor to the overall leak current in mammalian mitochondria incubated under physiological conditions at 37 °C, whereas proton slip increases at lower experimental temperature (Canton *et al.* 1995). Proton slip can also happen in association with the F-ATPase, in which the proton slips downhill across the pump to the matrix without contributing to ATP synthesis. In each case, proton slip is a property of the proton pump and increases with the pump turnover rate.
- **Electron leak and loosely coupled respiration:** Superoxide production by the ETS leads to a bypass of redox proton pumps and correspondingly lower $P \gg O_2$ ratio. This depends on the actual site of electron leak and the scavenging of hydrogen peroxide by cytochrome *c*, whereby electrons may re-enter the ETS with proton translocation by CIV.

- **Loss of compartmental integrity and acoupled respiration:** Electron transfer and catabolic O₂ flux proceed without compartmental proton translocation in disrupted mitochondrial fragments. Such fragments are an artefact of mitochondrial isolation, and may not fully fuse to re-establish structurally intact mitochondria. Loss of mtIM integrity, therefore, is the cause of acoupled respiration, which is a nonvectorial dissipative process without control by the protonmotive force.
- **Dyscoupled respiration:** Mitochondrial injuries may lead to *dyscoupling* as a pathological or toxicological cause of *uncoupled* respiration. Dyscoupling may involve any type of uncoupling mechanism, *e.g.*, opening the permeability transition pore. Dyscoupled respiration is distinguished from the experimentally induced *noncoupled* respiration in the ET-state (**Table 2**).

2.5.2. OXPHOS-state (Figure 5B): The OXPHOS-state is defined as the respiratory state with kinetically-saturating concentrations of O₂, respiratory and phosphorylation substrates, and absence of exogenous uncoupler, which provides an estimate of the maximal respiratory capacity in the OXPHOS-state for any given ET-pathway state. Respiratory capacities at kinetically-saturating substrate concentrations provide reference values or upper limits of performance, aiming at the generation of data sets for comparative purposes. Physiological activities and effects of substrate kinetics can be evaluated relative to the OXPHOS-capacity.

As discussed previously, 0.2 mM ADP does not fully saturate flux in isolated mitochondria (Gnaiger 2001; Puchowicz *et al.* 2004); greater [ADP] is required, particularly in permeabilized muscle fibres and cardiomyocytes, to overcome limitations by intracellular diffusion and by the reduced conductance of the mtOM (Jepihhina *et al.* 2011, Illaste *et al.* 2012, Simson *et al.* 2016), either through interaction with tubulin (Rostovtseva *et al.* 2008) or other intracellular structures (Birkedal *et al.* 2014). In addition, saturating ADP concentrations need to be evaluated under different experimental conditions such as temperature (Lemieux *et al.* 2017) and with different animal models (Blier and Guderley, 1993). In permeabilized muscle fibre bundles of high respiratory capacity, the apparent K_m for ADP increases up to 0.5 mM (Saks *et al.* 1998), consistent with experimental evidence that >90% saturation is reached only at >5 mM ADP (Pesta and Gnaiger 2012). Similar ADP concentrations are also required for accurate determination of OXPHOS-capacity in human clinical cancer samples and permeabilized cells (Klepinin *et al.* 2016; Koit *et al.* 2017). Whereas 2.5 to 5 mM ADP is sufficient to obtain the actual OXPHOS-capacity in many types of permeabilized tissue and cell preparations, experimental validation is required in each specific case.

2.5.3. Electron transfer-state (Figure 5C): O₂ flux determined in the ET-state yields an estimate of ET-capacity. The ET-state is defined as the *noncoupled* state with kinetically-saturating concentrations of O₂, respiratory substrate and optimum exogenous uncoupler concentration for maximum O₂ flux. Uncouplers are weak lipid-soluble acids which function as protonophores. These disrupt the barrier function of the mtIM and thus short circuit the protonmotive system, functioning like a clutch in a mechanical system. As a consequence of the nearly collapsed protonmotive force, the driving force is insufficient for phosphorylation, and $J_{P_s} = 0$. The most frequently used uncouplers are carbonyl cyanide *m*-chloro phenyl hydrazone (CCCP), carbonyl cyanide *p*-trifluoromethoxyphenylhydrazone (FCCP), or dinitrophenole (DNP). Stepwise titration of uncouplers stimulates respiration up to or above the level of O₂ consumption rates in the OXPHOS-state; respiration is inhibited, however, above optimum uncoupler concentrations (Mitchell 2011). Data obtained with a single dose of uncoupler must be evaluated with caution, particularly when a fixed uncoupler concentration is used in studies exploring a treatment or disease that may alter the mitochondrial content or mitochondrial sensitivity to inhibition by uncouplers. The effect on ET-capacity of the reversed function of F-ATPase (J_{P_r} ; **Figure 5C**) can be evaluated in the presence and absence of extramitochondrial ATP.

2.5.4. ROX state and *Rox*: Besides the three fundamental coupling states of mitochondrial preparations, the state of residual O₂ consumption, ROX, is relevant to assess respiratory function (**Figure 1**). ROX is not a coupling state. The rate of residual oxygen consumption, *Rox*, is defined as O₂ consumption due to oxidative reactions measured after inhibition of ET—with rotenone, malonic acid and antimycin A. Cyanide and azide inhibit not only CIV but catalase and several peroxidases involved in *Rox*. High concentrations of antimycin A, but not rotenone or cyanide, inhibit peroxisomal acyl-CoA oxidase and D-amino acid oxidase (Vamecq *et al.* 1987). *Rox* represents a baseline that is used to correct respiration measured in defined coupling states. *Rox*-corrected *L*, *P* and *E* not only lower the values of total fluxes, but also change the flux control ratios *L/P* and *L/E*. *Rox* is not necessarily equivalent to non-

767 mitochondrial reduction of O₂, considering O₂-consuming reactions in mitochondria that are not related
 768 to ET—such as O₂ consumption in reactions catalyzed by monoamine oxidases (type A and B),
 769 monoxygenases (cytochrome P450 monoxygenases), dioxygenase (sulfur dioxygenase and
 770 trimethyllysine dioxygenase), and several hydroxylases. Even isolated mitochondrial fractions,
 771 especially those obtained from liver, may be contaminated by peroxisomes. This fact makes the exact
 772 determination of mitochondrial O₂ consumption and mitochondria-associated generation of reactive
 773 oxygen species complicated (Schönfeld *et al.* 2009; Speijer 2016; **Figure 2**). The dependence of ROX-
 774 linked O₂ consumption needs to be studied in detail together with non-ET enzyme activities, availability
 775 of specific substrates, O₂ concentration, and electron leakage leading to the formation of reactive oxygen
 776 species.

777 **2.5.5. Quantitative relations:** E may exceed or be equal to P . $E > P$ is observed in many types
 778 of mitochondria, varying between species, tissues and cell types (Gnaiger 2009). $E - P$ is the excess ET-
 779 capacity pushing the phosphorylation-flux (**Figure 2C**) to the limit of its capacity of utilizing the
 780 protonmotive force. In addition, the magnitude of $E - P$ depends on the tightness of respiratory coupling
 781 or degree of uncoupling, since an increase of L causes P to increase towards the limit of E . The *excess*
 782 $E - P$ capacity, $E - P$, therefore, provides a sensitive diagnostic indicator of specific injuries of the
 783 phosphorylation-pathway, under conditions when E remains constant but P declines relative to controls
 784 (**Figure 4**). Substrate cocktails supporting simultaneous convergent electron transfer to the Q-junction
 785 for reconstitution of TCA cycle function establish pathway control states with high ET-capacity, and
 786 consequently increase the sensitivity of the $E - P$ assay.

787 E cannot theoretically be lower than P . $E < P$ must be discounted as an artefact, which may be
 788 caused experimentally by: (1) loss of oxidative capacity during the time course of the respirometric
 789 assay, since E is measured subsequently to P ; (2) using insufficient uncoupler concentrations; (3) using
 790 high uncoupler concentrations which inhibit ET (Gnaiger 2008); (4) high oligomycin concentrations
 791 applied for measurement of L before titrations of uncoupler, when oligomycin exerts an inhibitory effect
 792 on E . On the other hand, the excess ET-capacity is overestimated if non-saturating [ADP] or [P_i] are
 793 used. See State 3 in the next section.

794 The net OXPHOS-capacity is calculated by subtracting L from P (**Figure 4**). The net P»/O₂ equals
 795 P»/($P - L$), wherein the dissipative LEAK component in the OXPHOS-state may be overestimated. This
 796 can be avoided by measuring LEAK-respiration in a state when the protonmotive force is adjusted to its
 797 slightly lower value in the OXPHOS-state—by titration of an ET inhibitor (Divakaruni and Brand 2011).
 798 Any turnover-dependent components of proton leak and slip, however, are underestimated under these
 799 conditions (Garlid *et al.* 1993). In general, it is inappropriate to use the term *ATP production* or *ATP*
 800 *turnover* for the difference of O₂ flux measured in the OXPHOS and LEAK states. $P - L$ is the upper limit
 801 of OXPHOS-capacity that is freely available for ATP production (corrected for LEAK-respiration) and
 802 is fully coupled to phosphorylation with a maximum mechanistic stoichiometry (**Figure 4**).

803 The rates of LEAK respiration and OXPHOS capacity depend on (1) the tightness of coupling
 804 under the influence of the respiratory uncoupling mechanisms (**Figure 3**), and (2) the coupling
 805 stoichiometry, which varies as a function of the substrate type undergoing oxidation in ET-pathways
 806 with either two or three coupling sites (**Figure 2B**). When cocktails with NADH-linked substrates and
 807 succinate are used, the relative contribution of ET-pathways with three or two coupling sites cannot be
 808 controlled experimentally, is difficult to determine, and may shift in transitions between LEAK-,
 809 OXPHOS- and ET-states (Gnaiger 2014). Under these experimental conditions, we cannot separate the
 810 tightness of coupling *versus* coupling stoichiometry as the mechanisms of respiratory control in the shift
 811 of L/P ratios. The tightness of coupling and fully coupled O₂ flux, $P - L$ (**Table 2**), therefore, are obtained
 812 from measurements of coupling control of LEAK respiration, OXPHOS- and ET-capacities in well
 813 defined pathway states, using either pyruvate and malate as substrates or the classical succinate and
 814 rotenone substrate-inhibitor combination (**Figure 2B**).

815 **2.5.6. The steady-state:** Mitochondria represent a thermodynamically open system in non-
 816 equilibrium states of biochemical energy transformation. State variables (protonmotive force; redox
 817 states) and metabolic *rates* (fluxes) are measured in defined mitochondrial respiratory *states*. Steady-
 818 states can be obtained only in open systems, in which changes by internal transformations, *e.g.*, O₂
 819 consumption, are instantaneously compensated for by external fluxes, *e.g.*, O₂ supply, preventing a
 820 change of O₂ concentration in the system (Gnaiger 1993b). Mitochondrial respiratory states monitored
 821 in closed systems satisfy the criteria of pseudo-steady states for limited periods of time, when changes
 822 in the system (concentrations of O₂, fuel substrates, ADP, P_i, H⁺) do not exert significant effects on

823 metabolic fluxes (respiration, phosphorylation). Such pseudo-steady states require respiratory media
 824 with sufficient buffering capacity and substrates maintained at kinetically-saturating concentrations, and
 825 thus depend on the kinetics of the processes under investigation.

826

827 2.6. Classical terminology for isolated mitochondria

828 'When a code is familiar enough, it ceases appearing like a code; one forgets that there is a
 829 decoding mechanism. The message is identical with its meaning' (Hofstadter 1979).

830

831 Chance and Williams (1955; 1956) introduced five classical states of mitochondrial respiration
 832 and cytochrome redox states. **Table 3** shows a protocol with isolated mitochondria in a closed
 833 respirometric chamber, defining a sequence of respiratory states. States and rates are not specifically
 834 distinguished in this nomenclature.

835

836 **Table 3. Metabolic states of mitochondria (Chance and**
 837 **Williams, 1956; Table V).**

838

State	[O ₂]	ADP level	Substrate level	Respiration rate	Rate-limiting substance
1	>0	low	low	slow	ADP
2	>0	high	~0	slow	substrate
3	>0	high	high	fast	respiratory chain
4	>0	low	high	slow	ADP
5	0	high	high	0	oxygen

839

840

841 **2.6.1. State 1** is obtained after addition of isolated mitochondria to air-saturated
 842 isoosmotic/isotonic respiration medium containing P_i, but no fuel substrates and no adenylates, *i.e.*,
 843 AMP, ADP, ATP.

844 **2.6.2. State 2** is induced by addition of a 'high' concentration of ADP (typically 100 to 300 μM),
 845 which stimulates respiration transiently on the basis of endogenous fuel substrates and phosphorylates
 846 only a small portion of the added ADP. State 2 is then obtained at a low respiratory activity limited by
 847 exhausted endogenous fuel substrate availability (**Table 3**). If addition of specific inhibitors of
 848 respiratory complexes—such as rotenone—does not cause a further decline of O₂ flux, State 2 is
 849 equivalent to the ROX state (See below.). If inhibition is observed, undefined endogenous fuel substrates
 850 are a confounding factor of pathway control, contributing to the effect of subsequently externally added
 851 substrates and inhibitors. In contrast to the original protocol, an alternative sequence of titration steps is
 852 frequently applied, in which the alternative 'State 2' has an entirely different meaning, when this second
 853 state is induced by addition of fuel substrate without ADP or ATP (LEAK-state; in contrast to State 2
 854 defined in **Table 1** as a ROX state). Some researchers have called this condition as "pseudostate 4"
 855 because it has no significant concentrations of adenine nucleotides and hence it is not a near-
 856 physiological condition, although it should be used for calculating the net OXPHOS-capacity, *P-L*.

857 **2.6.3. State 3** is the state stimulated by addition of fuel substrates while the ADP concentration
 858 is still high (**Table 3**) and supports coupled energy transformation through oxidative phosphorylation.
 859 'High ADP' is a concentration of ADP specifically selected to allow the measurement of State 3 to State
 860 4 transitions of isolated mitochondria in a closed respirometric chamber. Repeated ADP titration re-
 861 establishes State 3 at 'high ADP'. Starting at O₂ concentrations near air-saturation (193 or 238 μM O₂
 862 at 37 °C or 25 °C and sea level at 1 atm or 101.32 kPa, and an oxygen solubility of respiration medium
 863 at 0.92 times that of pure water; Forstner and Gnaiger 1983), the total ADP concentration added must
 864 be low enough (typically 100 to 300 μM) to allow phosphorylation to ATP at a coupled O₂ flux that
 865 does not lead to O₂ depletion during the transition to State 4. In contrast, kinetically-saturating ADP
 866 concentrations usually are 10-fold higher than 'high ADP', *e.g.*, 2.5 mM in isolated mitochondria. The
 867 abbreviation State 3u is occasionally used in bioenergetics, to indicate the state of respiration after
 868 titration of an uncoupler, without sufficient emphasis on the fundamental difference between OXPHOS-
 869 capacity (*well-coupled* with an endogenous uncoupled component) and ET-capacity (*noncoupled*).

870 **2.6.4. State 4** is a LEAK-state that is obtained only if the mitochondrial preparation is intact and
 871 well-coupled. Depletion of ADP by phosphorylation to ATP causes a decline of O₂ flux in the transition
 872 from State 3 to State 4. Under the conditions of State 4, a maximum protonmotive force and high
 873 ATP/ADP ratio are maintained. The gradual decline of $Y_{P\gg/O_2}$ towards diminishing [ADP] at State 4 must
 874 be taken into account for calculation of $P\gg/O_2$ ratios (Gnaiger 2001). State 4 respiration, L_T (**Table 1**),
 875 reflects intrinsic proton leak and ATP hydrolysis activity. O₂ flux in State 4 is an overestimation of
 876 LEAK-respiration if the contaminating ATP hydrolysis activity recycles some ATP to ADP, $J_{P\ll}$, which
 877 stimulates respiration coupled to phosphorylation, $J_{P\gg} > 0$. Some degree of mechanical disruption and
 878 loss of mitochondrial integrity allows the exposed mitochondrial F-ATPases to hydrolyze the ATP
 879 synthesized by the fraction of coupled mitochondria. This can be tested by inhibition of the
 880 phosphorylation-pathway using oligomycin, ensuring that $J_{P\gg} = 0$ (State 4o). On the other hand, the State
 881 4 respiration reached after exhaustion of added ADP is a more physiological condition (*i.e.*, presence of
 882 ATP, ADP and even AMP). Sequential ADP titrations re-establish State 3, followed by State 3 to State
 883 4 transitions while sufficient O₂ is available. Anoxia may be reached, however, before exhaustion of
 884 ADP (State 5).

885 **2.6.5. State 5** is the state after exhaustion of O₂ in a closed respirometric chamber. Diffusion of
 886 O₂ from the surroundings into the aqueous solution may be a confounding factor preventing complete
 887 anoxia (Gnaiger 2001). Chance and Williams (1955) provide an alternative definition of State 5, which
 888 gives it the different meaning of ROX versus anoxia: ‘State 5 may be obtained by antimycin A treatment
 889 or by anaerobiosis’.

890 In **Table 3**, only States 3 and 4 are coupling control states, with the restriction that rates in State
 891 3 may be limited kinetically by non-saturating ADP concentrations.

892

893 2.7. Control and regulation

894

895 The terms metabolic *control* and *regulation* are frequently used synonymously, but are
 896 distinguished in metabolic control analysis: ‘We could understand the regulation as the mechanism that
 897 occurs when a system maintains some variable constant over time, in spite of fluctuations in external
 898 conditions (homeostasis of the internal state). On the other hand, metabolic control is the power to
 899 change the state of the metabolism in response to an external signal’ (Fell 1997). Respiratory control
 900 may be induced by experimental control signals that exert an influence on: (1) ATP demand and ADP
 901 phosphorylation-rate; (2) fuel substrate composition, pathway competition; (3) available amounts of
 902 substrates and O₂, *e.g.*, starvation and hypoxia; (4) the protonmotive force, redox states, flux–force
 903 relationships, coupling and efficiency; (5) Ca²⁺ and other ions including H⁺; (6) inhibitors, *e.g.*, nitric
 904 oxide or intermediary metabolites such as oxaloacetate; (7) signalling pathways and regulatory proteins,
 905 *e.g.*, insulin resistance, transcription factor hypoxia inducible factor 1.

906 Mechanisms of respiratory control and regulation include adjustments of: (1) enzyme activities
 907 by allosteric mechanisms and phosphorylation; (2) enzyme content, concentrations of cofactors and
 908 conserved moieties—such as adenylates, nicotinamide adenine dinucleotide [NAD⁺/NADH], coenzyme
 909 Q, cytochrome *c*; (3) metabolic channeling by supercomplexes; and (4) mitochondrial density (enzyme
 910 concentrations and membrane area) and morphology (cristae folding, fission and fusion). Mitochondria
 911 are targeted directly by hormones, *e.g.*, progesterone and glucacorticoids, which affect their energy
 912 metabolism (Lee *et al.* 2013; Gerö and Szabo 2016; Price and Dai 2016; Moreno *et al.* 2017).
 913 Evolutionary or acquired differences in the genetic and epigenetic basis of mitochondrial function (or
 914 dysfunction) between individuals; age; biological sex, and hormone concentrations; life style including
 915 exercise and nutrition; and environmental issues including thermal, atmospheric, toxic and
 916 pharmacological factors, exert an influence on all control mechanisms listed above. For reviews, see
 917 Brown 1992; Gnaiger 1993a, 2009; 2014; Paradies *et al.* 2014; Morrow *et al.* 2017.

918 Lack of control by a metabolic pathway, *e.g.*, phosphorylation-pathway, means that there will
 919 be no response to a variable activating it, *e.g.*, [ADP]. The reverse, however, is not true as the absence
 920 of a response to [ADP] does not exclude the phosphorylation-pathway from having some degree of
 921 control. The degree of control of a component of the OXPHOS-pathway on an output variable—such
 922 as O₂ flux, will in general be different from the degree of control on other outputs—such as
 923 phosphorylation-flux or proton leak flux. Therefore, it is necessary to be specific as to which input and
 924 output are under consideration (Fell 1997).

925 Respiratory control refers to the ability of mitochondria to adjust O₂ flux in response to external
 926 control signals by engaging various mechanisms of control and regulation. Respiratory control is
 927 monitored in a mitochondrial preparation under conditions defined as respiratory states, preferentially
 928 under near-physiological conditions of temperature, pH and medium ionic composition, to generate data
 929 of higher biological relevance. When phosphorylation of ADP to ATP is stimulated or depressed, an
 930 increase or decrease is observed in electron transfer measured as O₂ flux in respiratory coupling states
 931 of intact mitochondria ('controlled states' in the classical terminology of bioenergetics). Alternatively,
 932 coupling of electron transfer with phosphorylation is diminished by uncouplers. The corresponding
 933 coupling control state is characterized by a high respiratory rate without control by P» (noncoupled or
 934 'uncontrolled state').

935
 936

937 3. What is a rate?

938

939 The term *rate* is not adequately defined to be useful for reporting data. Normalization of 'rates'
 940 leads to a diversity of formats. Application of common and defined units is required for direct transfer
 941 of reported results into a database. The second [s] is the SI unit for the base quantity *time*. It is also the
 942 standard time-unit used in solution chemical kinetics.

943 The inconsistency of the meanings of rate becomes apparent when considering Galileo Galilei's
 944 famous principle, that 'bodies of different weight all fall at the same rate (have a constant acceleration)'
 945 (Coopersmith 2010). A rate may be an extensive quantity, which is a *flow*, *I*, when expressed per object
 946 (per number of cells or organisms) or per chamber (per system). 'System' is defined as the open or
 947 closed chamber of the measuring device. A rate is a *flux*, *J*, when expressed as a size-specific quantity
 948 (Figure 6A; Box 2).

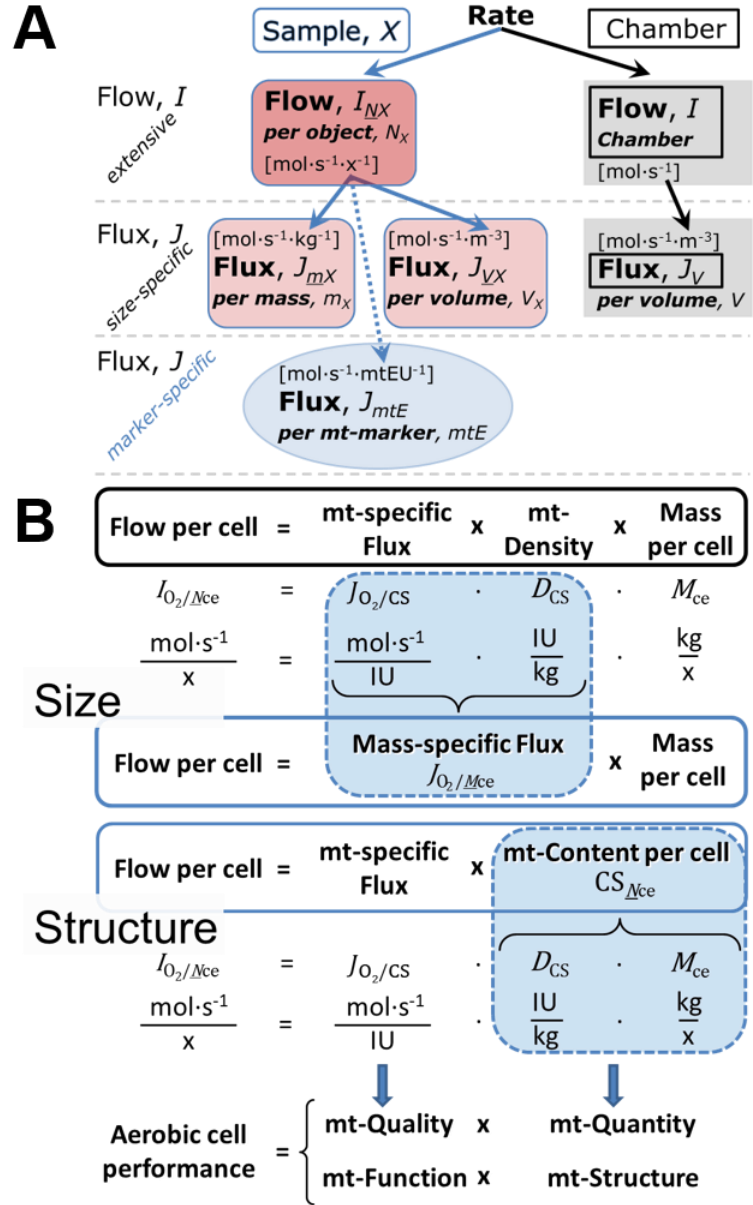
- 949 • **Extensive quantities:** An extensive quantity increases proportionally with system size. For
 950 example, mass and volume are extensive quantities. Flow is an extensive quantity. The
 951 magnitude of an extensive quantity is completely additive for non-interacting subsystems.
 952 The magnitude of these quantities depends on the extent or size of the system (Cohen *et al.*
 953 2008).
- 954 • **Size-specific quantities:** 'The adjective *specific* before the name of an extensive quantity is
 955 often used to mean *divided by mass*' (Cohen *et al.* 2008). In this system-paradigm, mass-
 956 specific flux is flow divided by mass of the system (the total mass of everything within the
 957 measuring chamber or reactor). Rates are frequently expressed as volume-specific flux. A
 958 mass-specific or volume-specific quantity is independent of the extent of non-interacting
 959 homogenous subsystems. Tissue-specific quantities (related to the *sample* in contrast to the
 960 *system*) are of fundamental interest in the field of comparative mitochondrial physiology,
 961 where *specific* refers to the *type of the sample* rather than *mass of the system*. The term
 962 *specific*, therefore, must be clarified; *sample-specific*, *e.g.*, muscle mass-specific
 963 normalization, is distinguished from *system-specific* quantities (mass or volume; Figure 6).
- 964 • **Intensive quantities:** In contrast to size-specific properties, forces are intensive quantities
 965 defined as the change of an extensive quantity per advancement of an energy transformation
 966 (Gnaiger 1993b).
- 967 • N_X and m_X indicate the number format and mass format, respectively, for expressing the
 968 quantity of a sample *X*. When different formats are indicated in symbols of derived quantities,
 969 the format (\underline{N} , \underline{m}) is shown as a subscript (*underlined italic*), as in $I_{O_2/\underline{N}X}$ and $J_{O_2/\underline{m}X}$. Oxygen
 970 flow and flux are expressed in the molar format, n_{O_2} [mol], but in the volume format, V_{O_2} [m³]
 971 in ergometry. For mass-specific flux these formats can be distinguished as $J_{nO_2/\underline{m}X}$ and $J_{VO_2/\underline{m}X}$,
 972 respectively. Further examples are given in Figure 6 and Table 4.

973

974 **Figure 6. Flow and flux, and**
 975 **normalization in structure-**
 976 **function analysis**

977 (A) When expressing metabolic
 978 ‘rate’ measured in a chamber, a
 979 fundamental distinction is made
 980 between relating the rate to the
 981 experimental sample (left) or
 982 chamber (right). The different
 983 meanings of rate need to be
 984 specified by the chosen
 985 normalization. Left: Results are
 986 expressed as mass-specific flux, J_{mX} ,
 987 per mg protein, dry or wet mass.
 988 Cell volume, V_{ce} , may be used for
 989 normalization (volume-specific
 990 flux, J_{Vce}). Right: Flow per chamber,
 991 I , or flux per chamber volume, J_V ,
 992 are merely reported for
 993 methodological reasons.

994 (B) O_2 flow per cell, $I_{O_2/Nce}$, is the
 995 product of mitochondria-specific
 996 flux, mt-density and mass per cell.
 997 Unstructured analysis: performance
 998 is the product of mass-specific flux,
 999 $J_{O_2/MX}$ [$\text{mol}\cdot\text{s}^{-1}\cdot\text{kg}^{-1}$], and size
 1000 (mass per cell). Structured analysis:
 1001 performance is the product of
 1002 mitochondrial function (mt-specific
 1003 flux) and structure (mt-content).
 1004 Modified from Gnaiger (2014). For
 1005 further details see **Table 4**.



1011 **Box 2: Metabolic flows and fluxes: vectoral, vectorial, and scalar**

1012
 1013 In a generalization of electrical terms, flow as an extensive quantity (I ; per system) is
 1014 distinguished from flux as a size-specific quantity (J ; per system size). *Flows*, I_{tr} , are defined for all
 1015 transformations as extensive quantities. Electric charge per unit time is electric flow or current, $I_{el} =$
 1016 $dQ_{el} \cdot dt^{-1}$ [$A \equiv C \cdot s^{-1}$]. When dividing I_{el} by size of the system (cross-sectional area of a ‘wire’), we obtain
 1017 flux as a size-specific quantity, which is the current density (surface-density of flow) perpendicular to
 1018 the direction of flux, $J_{el} = I_{el} \cdot A^{-1}$ [$A \cdot m^{-2}$] (Cohen et al. 2008). Fluxes with *spatial* geometric direction and
 1019 magnitude are *vectors*. Vector and scalar *fluxes* are related to flows as $J_{tr} = I_{tr} \cdot A^{-1}$ [$\text{mol}\cdot\text{s}^{-1}\cdot\text{m}^{-2}$] and $J_{tr} =$
 1020 $I_{tr} \cdot V^{-1}$ [$\text{mol}\cdot\text{s}^{-1}\cdot\text{m}^{-3}$], expressing flux as an area-specific vector or volume-specific vectorial or scalar
 1021 quantity, respectively (Gnaiger 1993b). We use the metre–kilogram–second–ampere (MKSA)
 1022 international system of units (SI) for general cases ([m], [kg], [s] and [A]), with decimal SI prefixes for
 1023 specific applications (**Table 4**).

1024 We suggest to define: (1) *vectoral* fluxes, which are translocations as functions of *gradients* with
 1025 direction in geometric space in continuous systems; (2) *vectorial* fluxes, which describe translocations
 1026 in discontinuous systems and are restricted to information on *compartmental differences*
 1027 (transmembrane proton flux); and (3) *scalar* fluxes, which are transformations in a *homogenous* system
 1028 (catabolic O_2 flux, J_{kO_2}).

1029 **4. Normalization of rate per sample**

1030

1031 The challenges of measuring mitochondrial respiratory flux are matched by those of
 1032 normalization. Normalization (**Table 4**) is guided by physicochemical principles, methodological
 1033 considerations, and conceptual strategies (**Figure 6**).

1034

1035 **Table 4. Sample concentrations and normalization of flux.**

1036

Expression	Symbol	Definition	Unit	Notes
Sample				
identity of sample	X	object: cell, tissue, animal, patient		
number of sample entities X	N_X	number of objects	x	1
mass of sample X	m_X		kg	2
mass of object X	M_X	$M_X = m_X \cdot N_X^{-1}$	$\text{kg} \cdot \text{x}^{-1}$	2
Mitochondria				
mitochondria	mt	$X = \text{mt}$		
amount of mt-elementary components	mtE	quantity of mt-marker	mtEU	
Concentrations				
object number concentration	C_{NX}	$C_{NX} = N_X \cdot V^{-1}$	$\text{x} \cdot \text{m}^{-3}$	3
sample mass concentration	C_{mX}	$C_{mX} = m_X \cdot V^{-1}$	$\text{kg} \cdot \text{m}^{-3}$	
mitochondrial concentration	C_{mtE}	$C_{mtE} = mtE \cdot V^{-1}$	$\text{mtEU} \cdot \text{m}^{-3}$	4
specific mitochondrial density	D_{mtE}	$D_{mtE} = mtE \cdot m_X^{-1}$	$\text{mtEU} \cdot \text{kg}^{-1}$	5
mitochondrial content, mtE per object X	mtE_{NX}	$mtE_{NX} = mtE \cdot N_X^{-1}$	$\text{mtEU} \cdot \text{x}^{-1}$	6
O₂ flow and flux				
flow, system	I_{O_2}	internal flow	$\text{mol} \cdot \text{s}^{-1}$	7
volume-specific flux	J_{V,O_2}	$J_{V,O_2} = I_{O_2} \cdot V^{-1}$	$\text{mol} \cdot \text{s}^{-1} \cdot \text{m}^{-3}$	8
flow per object X	$I_{O_2/NX}$	$I_{O_2/NX} = J_{V,O_2} \cdot C_{NX}^{-1}$	$\text{mol} \cdot \text{s}^{-1} \cdot \text{x}^{-1}$	9
mass-specific flux	$J_{O_2/mX}$	$J_{O_2/mX} = J_{V,O_2} \cdot C_{mX}^{-1}$	$\text{mol} \cdot \text{s}^{-1} \cdot \text{kg}^{-1}$	10
mt-marker-specific flux	$J_{O_2/mtE}$	$J_{O_2/mtE} = J_{V,O_2} \cdot C_{mtE}^{-1}$	$\text{mol} \cdot \text{s}^{-1} \cdot \text{mtEU}^{-1}$	11

1037 1 The unit x for a number is not used by IUPAC. To avoid confusion, the units [$\text{kg} \cdot \text{x}^{-1}$] and [kg]
 1038 distinguish the mass per object from the mass of a sample that may contain any number of objects.
 1039 Similarly, the units for flow per system *versus* flow per object are [$\text{mol} \cdot \text{s}^{-1}$] (Note 8) and [$\text{mol} \cdot \text{s}^{-1} \cdot \text{x}^{-1}$]
 1040 (Note 10).

1041 2 Units are given in the MKSA system (**Box 2**). The *SI* prefix k is used for the *SI* base unit of mass (kg
 1042 = 1,000 g). In praxis, various *SI* prefixes are used for convenience, to make numbers easily readable,
 1043 e.g., 1 mg tissue, cell or mitochondrial mass instead of 0.000001 kg.

1044 3 In case of cells (sample $X = \text{cells}$), the object number concentration is $C_{N_{ce}} = N_{ce} \cdot V^{-1}$, and volume
 1045 may be expressed in [$\text{dm}^3 \equiv \text{L}$] or [$\text{cm}^3 = \text{mL}$]. See **Table 5** for different object types.

1046 4 mt-concentration is an experimental variable, dependent on sample concentration: (1) $C_{mtE} = mtE \cdot V^{-1}$;
 1047 (2) $C_{mtE} = mtE_X \cdot C_{NX}$; (3) $C_{mtE} = C_{mX} \cdot D_{mtE}$.

1048 5 If the amount of mitochondria, mtE , is expressed as mitochondrial mass, then D_{mtE} is the mass
 1049 fraction of mitochondria in the sample. If mtE is expressed as mitochondrial volume, V_{mt} , and the
 1050 mass of sample, m_X , is replaced by volume of sample, V_X , then D_{mtE} is the volume fraction of
 1051 mitochondria in the sample.

1052 6 $mtE_{NX} = mtE \cdot N_X^{-1} = C_{mtE} \cdot C_{NX}^{-1}$.

1053 7 O_2 can be replaced by other chemicals to study different reactions, e.g., ATP, H_2O_2 , or vesicular
 1054 compartmental translocations, e.g., Ca^{2+} .

- 1055 8 I_{O_2} and V are defined per instrument chamber as a system of constant volume (and constant
 1056 temperature), which may be closed or open. I_{O_2} is abbreviated for I_{rO_2} , *i.e.*, the metabolic or internal
 1057 O_2 flow of the chemical reaction r in which O_2 is consumed, hence the negative stoichiometric
 1058 number, $\nu_{O_2} = -1$. $I_{rO_2} = d_r n_{O_2} / dt \cdot \nu_{O_2}^{-1}$. If r includes all chemical reactions in which O_2 participates, then
 1059 $d_r n_{O_2} = dn_{O_2} - d_e n_{O_2}$, where dn_{O_2} is the change in the amount of O_2 in the instrument chamber and $d_e n_{O_2}$
 1060 is the amount of O_2 added externally to the system. At steady state, by definition $dn_{O_2} = 0$, hence $d_r n_{O_2}$
 1061 $= -d_e n_{O_2}$. Note that in this context ‘external’, e , refers to the system, whereas in Figure 1 ‘external’,
 1062 ext , refers to the organism.
 1063 9 J_{V,O_2} is an experimental variable, expressed per volume of the instrument chamber.
 1064 10 $I_{O_2/NX}$ is a physiological variable, depending on the size of entity X .
 1065 11 There are many ways to normalize for a mitochondrial marker, that are used in different experimental
 1066 approaches: (1) $J_{O_2/mtE} = J_{V,O_2} \cdot C_{mtE}^{-1}$; (2) $J_{O_2/mtE} = J_{V,O_2} \cdot C_{mX}^{-1} \cdot D_{mtE}^{-1} = J_{O_2/mX} \cdot D_{mtE}^{-1}$; (3) $J_{O_2/mtE} =$
 1067 $J_{V,O_2} \cdot C_{NX}^{-1} \cdot mtE_{NX}^{-1} = I_{O_2/NX} \cdot mtE_{NX}^{-1}$; (4) $J_{O_2/mtE} = I_{O_2} \cdot mtE^{-1}$. The mt-elementary unit [mtEU] varies depending
 1068 on the mt-marker.
 1069
 1070
 1071

Table 5. Sample types, X, abbreviations, and quantification.

Identity of sample	X	N_X	Mass ^a	Volume	mt-Marker
mitochondrial preparation		[x]	[kg]	[m ³]	[mtEU]
isolated mitochondria	imt		m_{mt}	V_{mt}	mtE
tissue homogenate	thom		m_{thom}		mtE_{thom}
permeabilized tissue	pti		m_{pti}		mtE_{pti}
permeabilized fibre	pfi		m_{pfi}		mtE_{pfi}
permeabilized cell	pce	N_{pce}	M_{pce}	V_{pce}	mtE_{pce}
cells ^b	ce	N_{ce}	M_{ce}	V_{ce}	mtE_{ce}
intact cell, viable cell	vce	N_{vce}	M_{vce}	V_{vce}	
dead cell	dce	N_{dce}	M_{dce}	V_{dce}	
organism	org	N_{org}	M_{org}	V_{org}	

^a Instead of mass, the wet weight or dry weight is frequently stated, W_w or W_d . m_X is mass of the sample [kg], M_X is mass of the object [kg·x⁻¹] (Table 4).

^b Total cell count, $N_{ce} = N_{vce} + N_{dce}$

4.1. Flow: per object

4.1.1. Number concentration, C_{NX} : Normalization per sample concentration is routinely required to report respiratory data. C_{NX} is the experimental number concentration of sample X . In the case of animals, *e.g.*, nematodes, $C_{NX} = N_X/V$ [x·L⁻¹], where N_X is the number of organisms in the chamber. Similarly, the number of cells per chamber volume is the number concentration of permeabilized or intact cells $C_{Nce} = N_{ce}/V$ [x·L⁻¹], where N_{ce} is the number of cells in the chamber (Table 4).

4.1.2. Flow per object, $I_{O_2/NX}$: O_2 flow per cell is calculated from volume-specific O_2 flux, J_{V,O_2} [nmol·s⁻¹·L⁻¹] (per V of the measurement chamber [L]), divided by the number concentration of cells. The total cell count is the sum of viable and dead cells, $N_{ce} = N_{vce} + N_{dce}$ (Table 5). The cell viability index, $VI = N_{vce}/N_{ce}$, is the ratio of viable cells (N_{vce} ; before experimental permeabilization) per total cell count. After experimental permeabilization, all cells are permeabilized, $N_{pce} = N_{ce}$. The cell viability index can be used to normalize respiration for the number of cells that have been viable before experimental permeabilization, $I_{O_2/Nvce} = I_{O_2/Nce}/VI$, considering that mitochondrial respiratory dysfunction in dead cells should be eliminated as a confounding factor.

The complexity changes when the object is a whole organism studied as an experimental model. The scaling law in respiratory physiology reveals a strong interaction between O_2 flow and individual body mass: *basal* metabolic rate (flow) does not increase linearly with body mass, whereas *maximum* mass-specific O_2 flux, \dot{V}_{O_2max} or \dot{V}_{O_2peak} , is approximately constant across a large range of individual body mass (Weibel and Hoppeler 2005). Individuals, breeds and species, however, deviate substantially from this relationship. \dot{V}_{O_2peak} of human endurance athletes is 60 to 80 mL O_2 ·min⁻¹·kg⁻¹ body mass, converted to $J_{O_2peak/Morg}$ of 45 to 60 nmol·s⁻¹·g⁻¹ (Gnaiger 2014; Table 6).

4.2. Size-specific flux: per sample size

4.2.1. Sample concentration, C_{mX} : Considering permeabilized tissue, homogenate or cells as the sample, X , the sample mass is m_X [mg], which is frequently measured as wet or dry weight, W_w or W_d [mg], respectively, or as amount of protein, m_{Protein} . The sample concentration is the mass of the subsample per volume of the measurement chamber, $C_{mX} = m_X/V$ [$\text{g}\cdot\text{L}^{-1} = \text{mg}\cdot\text{mL}^{-1}$]. X is the type of sample—isolated mitochondria, tissue homogenate, permeabilized fibres or cells (**Table 5**).

4.2.2. Size-specific flux: Cellular O_2 flow can be compared between cells of identical size. To take into account changes and differences in cell size, normalization is required to obtain cell size-specific or mitochondrial marker-specific O_2 flux (Renner *et al.* 2003).

- **Mass-specific flux, $J_{\text{O}_2/mX}$ [$\text{mol}\cdot\text{s}^{-1}\cdot\text{kg}^{-1}$]:** Mass-specific flux is obtained by expressing respiration per mass of sample, m_X [mg]. Flow per cell is divided by mass per cell, $J_{\text{O}_2/mce} = I_{\text{O}_2/Nce}/M_{Nce}$. Or chamber volume-specific flux, J_{V,O_2} , is divided by mass concentration of X in the chamber, $J_{\text{O}_2/mX} = J_{V,\text{O}_2}/C_{mX}$.
- **Cell volume-specific flux, $J_{\text{O}_2/VX}$ [$\text{mol}\cdot\text{s}^{-1}\cdot\text{m}^{-3}$]:** Sample volume-specific flux is obtained by expressing respiration per volume of sample. For example, in the case of using cells as sample will be the volume of cells added to the chamber (**Figure 6**).

If size-specific O_2 flux is constant and independent of sample size, then there is no interaction between the subsystems. For example, a 1.5 mg and a 3.0 mg muscle sample respire at identical mass-specific flux. Mass-specific O_2 flux, however, may change with the mass of a tissue sample, cells or isolated mitochondria in the measuring chamber, in which the nature of the interaction becomes an issue. Therefore, cell density must be optimized, particularly in experiments carried out in wells, considering the confluency of the cell monolayer or clumps of cells (Salabei *et al.* 2014).

4.3. Marker-specific flux: per mitochondrial content

Tissues can contain multiple cell populations that may have distinct mitochondrial subtypes. Mitochondria undergo dynamic fission and fusion cycles, and can exist in multiple stages and sizes that may be altered by a range of factors. The isolation of mitochondria (often achieved through differential centrifugation) can therefore yield a subsample of the mitochondrial types present in a tissue, depending on the isolation protocols utilized (*e.g.*, centrifugation speed). This possible bias should be taken into account when planning experiments using isolated mitochondria. Different sizes of mitochondria are enriched at specific centrifugation speeds, which can be used strategically for isolation of mitochondrial subpopulations.

Part of the mitochondrial content of a tissue is lost during preparation of isolated mitochondria. The fraction of isolated mitochondria obtained from a tissue sample is expressed as mitochondrial recovery. At a high mitochondrial recovery the fraction of isolated mitochondria is more representative of the total mitochondrial population than in preparations characterized by low recovery. Determination of the mitochondrial recovery and yield is based on measurement of the concentration of a mitochondrial marker in the stock of isolated mitochondria, $C_{mtE,\text{stock}}$, and crude tissue homogenate, $C_{mtE,\text{thom}}$, which simultaneously provides information on the specific mitochondrial density in the sample, D_{mtE} (**Table 4**).

When discussing concepts on normalization, it is essential to consider the question of the study. If the study aims at comparing tissue performance—such as the effects of a treatment on a specific tissue, then normalization for tissue mass or protein content is appropriate. However, if the aim is to find differences on mitochondrial function independent of mitochondrial density (**Table 4**), then normalization to a mitochondrial marker is imperative (**Figure 6**). One cannot assume that quantitative changes in various markers—such as mitochondrial proteins—necessarily occur in parallel with one another. It should be established that the marker chosen is not selectively altered by the performed treatment. In conclusion, the normalization must reflect the question under investigation to reach a satisfying answer. On the other hand, the goal of comparing results across projects and institutions requires standardization on normalization for entry into a databank.

4.3.1. Mitochondrial concentration, C_{mtE} , and mitochondrial markers: Mitochondrial organelles comprise a dynamic cellular reticulum in various states of fusion and fission. Hence, the definition of an "amount" of mitochondria is often misconceived: mitochondria cannot be counted reliably as a number of occurring elementary components. Therefore, quantification of the "amount" of

1154 mitochondria depends on the measurement of chosen mitochondrial markers. ‘Mitochondria are the
 1155 structural and functional elementary units of cell respiration’ (Gnaiger 2014). The quantity of a
 1156 mitochondrial marker can reflect the amount of *mitochondrial elementary components*, mtE , expressed
 1157 in various mitochondrial elementary units [mtEU] specific for each measured mt-marker (**Table 4**).
 1158 However, since mitochondrial quality may change in response to stimuli—particularly in mitochondrial
 1159 dysfunction (Campos *et al.* 2017) and after exercise training (Pesta *et al.* 2011) and during aging (Daum
 1160 *et al.* 2013)—some markers can vary while others are unchanged: (1) Mitochondrial volume and
 1161 membrane area are structural markers, whereas mitochondrial protein mass is commonly used as a
 1162 marker for isolated mitochondria. (2) Molecular and enzymatic mitochondrial markers (amounts or
 1163 activities) can be selected as matrix markers, *e.g.*, citrate synthase activity, mtDNA; mtIM-markers, *e.g.*,
 1164 cytochrome *c* oxidase activity, aa_3 content, cardiolipin, or mtOM-markers, *e.g.*, the voltage-dependent
 1165 anion channel (VDAC), TOM20. (3) Extending the measurement of mitochondrial marker enzyme
 1166 activity to mitochondrial pathway capacity, ET- or OXPHOS-capacity can be considered as an
 1167 integrative functional mitochondrial marker.

1168 Depending on the type of mitochondrial marker, the mitochondrial elementary component, mtE ,
 1169 is expressed in marker-specific units. Mitochondrial concentration in the measurement chamber and the
 1170 tissue of origin are quantified as (1) a quantity for normalization in functional analyses, C_{mtE} , and (2) a
 1171 physiological output that is the result of mitochondrial biogenesis and degradation, D_{mtE} , respectively
 1172 (**Table 4**). It is recommended, therefore, to distinguish *experimental mitochondrial concentration*, C_{mtE}
 1173 $= mtE/V$ and *physiological mitochondrial density*, $D_{mtE} = mtE/m_X$. Then mitochondrial density is the
 1174 amount of mitochondrial elementary components per mass of tissue, which is a biological variable
 1175 (**Figure 6**). The experimental variable is mitochondrial density multiplied by sample mass concentration
 1176 in the measuring chamber, $C_{mtE} = D_{mtE} \cdot C_{m_X}$, or mitochondrial content multiplied by sample number
 1177 concentration, $C_{mtE} = mtE_X \cdot C_{N_X}$ (**Table 4**).

1178 **4.3.2. mt-Marker-specific flux, $J_{O_2/mtE}$:** Volume-specific metabolic O_2 flux depends on: (1) the
 1179 sample concentration in the volume of the instrument chamber, C_{m_X} , or C_{N_X} ; (2) the mitochondrial
 1180 density in the sample, $D_{mtE} = mtE/m_X$ or $mtE_X = mtE/N_X$; and (3) the specific mitochondrial activity or
 1181 performance per elementary mitochondrial unit, $J_{O_2/mtE} = J_{V,O_2}/C_{mtE}$ [$\text{mol} \cdot \text{s}^{-1} \cdot \text{mtEU}^{-1}$] (**Table 4**).
 1182 Obviously, the numerical results for $J_{O_2/mtE}$ vary with the type of mitochondrial marker chosen for
 1183 measurement of mtE and $C_{mtE} = mtE/V$ [$\text{mtEU} \cdot \text{m}^{-3}$].

1184 Different methods are implicated in the quantification of mitochondrial markers and have
 1185 different strengths. Some problems are common for all mitochondrial markers, mtE : (1) Accuracy of
 1186 measurement is crucial, since even a highly accurate and reproducible measurement of O_2 flux results
 1187 in an inaccurate and noisy expression if normalized by a biased and noisy measurement of a
 1188 mitochondrial marker. This problem is acute in mitochondrial respiration because the denominators used
 1189 (the mitochondrial markers) are often small moieties of which accurate and precise determination is
 1190 difficult. This problem can be avoided when O_2 fluxes measured in substrate-uncoupler-inhibitor
 1191 titration protocols are normalized for flux in a defined respiratory reference state, which is used as an
 1192 *internal* marker and yields flux control ratios, *FCRs*. *FCRs* are independent of externally measured
 1193 markers and, therefore, are statistically robust, considering the limitations of ratios in general (Jasienski
 1194 and Bazzaz 1999). *FCRs* indicate qualitative changes of mitochondrial respiratory control, with highest
 1195 quantitative resolution, separating the effect of mitochondrial density or concentration on J_{O_2/m_X} and
 1196 I_{O_2/N_X} from that of function per elementary mitochondrial marker, $J_{O_2/mtE}$ (Pesta *et al.* 2011; Gnaiger
 1197 2014). (2) If mitochondrial quality does not change and only the amount of mitochondria varies as a
 1198 determinant of mass-specific flux, any marker is equally qualified in principle; then in practice selection
 1199 of the optimum marker depends only on the accuracy and precision of measurement of the mitochondrial
 1200 marker. (3) If mitochondrial flux control ratios change, then there may not be any best mitochondrial
 1201 marker. In general, measurement of multiple mitochondrial markers enables a comparison and
 1202 evaluation of normalization for a variety of mitochondrial markers. Particularly during postnatal
 1203 development, the activity of marker enzymes—such as cytochrome *c* oxidase and citrate synthase—
 1204 follows different time courses (Drahota *et al.* 2004). Evaluation of mitochondrial markers in healthy
 1205 controls is insufficient for providing guidelines for application in the diagnosis of pathological states
 1206 and specific treatments.

1207 In line with the concept of the respiratory control ratio (Chance and Williams 1955a), the most
 1208 readily used normalization is that of flux control ratios and flux control factors (Gnaiger 2014). Selection
 1209 of the state of maximum flux in a protocol as the reference state has the advantages of: (1) internal

1210 normalization; (2) statistically validated linearization of the response in the range of 0 to 1; and (3)
 1211 consideration of maximum flux for integrating a large number of elementary steps in the OXPHOS- or
 1212 ET-pathways. This reduces the risk of selecting a functional marker that is specifically altered by the
 1213 treatment or pathology, yet increases the chance that the highly integrative pathway is disproportionately
 1214 affected, *e.g.*, the OXPHOS- rather than ET-pathway in case of an enzymatic defect in the
 1215 phosphorylation-pathway. In this case, additional information can be obtained by reporting flux control
 1216 ratios based on a reference state which indicates stable tissue-mass specific flux.

1217 Stereological determination of mitochondrial content via two-dimensional transmission electron
 1218 microscopy can have limitations due to the dynamics of mitochondrial size (Meinild Lundby *et al.*
 1219 2017). Accurate determination of three-dimensional volume by two-dimensional microscopy can be
 1220 both time consuming and statistically challenging (Larsen *et al.* 2012).

1221 The validity of using mitochondrial marker enzymes (citrate synthase activity, CI to CIV amount
 1222 or activity) for normalization of flux is limited in part by the same factors that apply to flux control
 1223 ratios. Strong correlations between various mitochondrial markers and citrate synthase activity
 1224 (Reichmann *et al.* 1985; Boushel *et al.* 2007; Mogensen *et al.* 2007) are expected in a specific tissue of
 1225 healthy persons and in disease states not specifically targeting citrate synthase. Citrate synthase activity
 1226 is acutely modifiable by exercise (Tonkonogi *et al.* 1997; Leek *et al.* 2001). Evaluation of mitochondrial
 1227 markers related to a selected age and sex cohort cannot be extrapolated to provide recommendations for
 1228 normalization in respirometric diagnosis of disease, in different states of development and ageing,
 1229 different cell types, tissues, and species. mtDNA normalized to nDNA via qPCR is correlated to
 1230 functional mitochondrial markers including OXPHOS- and ET-capacity in some cases (Puntschart *et al.*
 1231 1995; Wang *et al.* 1999; Menshikova *et al.* 2006; Boushel *et al.* 2007; Ehinger *et al.* 2015), but lack of
 1232 such correlations have been reported (Menshikova *et al.* 2005; Schultz and Wiesner 2000; Pesta *et al.*
 1233 2011). Several studies indicate a strong correlation between cardiolipin content and increase in
 1234 mitochondrial function with exercise (Menshikova *et al.* 2005; Menshikova *et al.* 2007; Larsen *et al.*
 1235 2012; Faber *et al.* 2014), but it has not been evaluated as a general mitochondrial biomarker in disease.
 1236 With no single best mitochondrial marker, a good strategy is to quantify several different biomarkers to
 1237 minimize the decorrelating effects caused by diseases, treatments, or other factors. Determination of
 1238 multiple markers, particularly a matrix marker and a marker from the mtIM, allows tracking changes in
 1239 mitochondrial quality defined by their ratio.

1240
 1241

1242 5. Normalization of rate per system

1243

1244 5.1. Flow: per chamber

1245

1246 The experimental system (experimental chamber) is part of the measurement instrument,
 1247 separated from the environment as an isolated, closed, open, isothermal or non-isothermal system
 1248 (Table 4). Reporting O₂ flows per respiratory chamber, I_{O_2} [nmol·s⁻¹], restricts the analysis to intra-
 1249 experimental comparison of relative differences.

1250

1251 5.2. Flux: per chamber volume

1252

1253 **5.2.1. System-specific flux, J_{V,O_2} :** We distinguish between (1) the *system* with volume V and mass
 1254 m defined by the system boundaries, and (2) the *sample* or *objects* with volume V_X and mass m_X that are
 1255 enclosed in the experimental chamber (Figure 6). Metabolic O₂ flow per object, I_{O_2/N_X} , is the total O₂
 1256 flow in the system divided by the number of objects, N_X , in the system. I_{O_2/N_X} increases as the mass of
 1257 the object is increased. Sample mass-specific O₂ flux, J_{O_2/m_X} should be independent of the mass of the
 1258 sample studied in the instrument chamber, but system volume-specific O₂ flux, J_{V,O_2} (per volume of the
 1259 instrument chamber), increases in proportion to the mass of the sample in the chamber. Whereas J_{V,O_2}
 1260 depends on mass-concentration of the sample in the chamber, it should be independent of the chamber
 1261 (system) volume at constant sample mass. There are practical limitations to increase the mass-
 1262 concentration of the sample in the chamber, when one is concerned about crowding effects and
 1263 instrumental time resolution.

1264 **5.2.2. Advancement per volume:** When the reactor volume does not change during the reaction,
 1265 which is typical for liquid phase reactions, the volume-specific flux of a chemical reaction r is the time

1266 derivative of the advancement of the reaction per unit volume, $J_{V,rB} = d_r \xi_B / dt \cdot V^{-1}$ [(mol·s⁻¹)·L⁻¹]. The *rate*
 1267 *of concentration change* is dc_B/dt [(mol·L⁻¹)·s⁻¹], where concentration is $c_B = n_B/V$. There is a difference
 1268 between (1) J_{V,rO_2} [mol·s⁻¹·L⁻¹] and (2) rate of concentration change [mol·L⁻¹·s⁻¹]. These merge to a single
 1269 expression only in closed systems. In open systems, internal transformations (catabolic flux, O₂
 1270 consumption) are distinguished from external flux (such as O₂ supply). External fluxes of all substances
 1271 are zero in closed systems. In a closed chamber O₂ consumption (internal flux of catabolic reactions k),
 1272 I_{kO_2} [pmol·s⁻¹], causes a decline of the amount of O₂ in the system, n_{O_2} [nmol]. Normalization of these
 1273 quantities for the volume of the system, V [L \equiv dm³], yields volume-specific O₂ flux, $J_{V,kO_2} = I_{kO_2}/V$
 1274 [nmol·s⁻¹·L⁻¹], and O₂ concentration, [O₂] or $c_{O_2} = n_{O_2}/V$ [μ mol·L⁻¹ = μ M = nmol·mL⁻¹]. Instrumental
 1275 background O₂ flux is due to external flux into a non-ideal closed respirometer; then total volume-
 1276 specific flux has to be corrected for instrumental background O₂ flux—O₂ diffusion into or out of the
 1277 instrumental chamber. J_{V,kO_2} is relevant mainly for methodological reasons and should be compared with
 1278 the accuracy of instrumental resolution of background-corrected flux, *e.g.*, ± 1 nmol·s⁻¹·L⁻¹ (Gnaiger
 1279 2001). ‘Metabolic’ or catabolic indicates O₂ flux, J_{kO_2} , corrected for: (1) instrumental background O₂
 1280 flux; (2) chemical background O₂ flux due to autoxidation of chemical components added to the
 1281 incubation medium; and (3) *Rox* for O₂-consuming side reactions unrelated to the catabolic pathway k .

1282
1283

1284 6. Conversion of units

1285

1286 Many different units have been used to report the O₂ consumption rate, OCR (Table 6). SI base
 1287 units provide the common reference to introduce the theoretical principles (Figure 6), and are used with
 1288 appropriately chosen *SI* prefixes to express numerical data in the most practical format, with an effort
 1289 towards unification within specific areas of application (Table 7). Reporting data in *SI* units—including
 1290 the mole [mol], coulomb [C], joule [J], and second [s]—should be encouraged, particularly by journals
 1291 which propose the use of *SI* units.

1292

1293 **Table 6. Conversion of various formats and units used in respirometry and**
 1294 **ergometry.** e^- is the number of electrons or reducing equivalents. z_B is the charge number
 1295 of entity B.
 1296

Format	1 Unit		Multiplication factor	<i>SI</i> -unit	Notes
\underline{n}	ng.atom O·s ⁻¹	(2 e^-)	0.5	nmol O ₂ ·s ⁻¹	
\underline{n}	ng.atom O·min ⁻¹	(2 e^-)	8.33	pmol O ₂ ·s ⁻¹	
\underline{n}	natom O·min ⁻¹	(2 e^-)	8.33	pmol O ₂ ·s ⁻¹	
\underline{n}	nmol O ₂ ·min ⁻¹	(4 e^-)	16.67	pmol O ₂ ·s ⁻¹	
\underline{n}	nmol O ₂ ·h ⁻¹	(4 e^-)	0.2778	pmol O ₂ ·s ⁻¹	
\underline{V} to \underline{n}	mL O ₂ ·min ⁻¹ at STPD ^a		0.744	μ mol O ₂ ·s ⁻¹	1
\underline{e} to \underline{n}	W = J/s at -470 kJ/mol O ₂		-2.128	μ mol O ₂ ·s ⁻¹	
\underline{e} to \underline{n}	mA = mC·s ⁻¹	($z_{H^+} = 1$)	10.36	nmol H ⁺ ·s ⁻¹	2
\underline{e} to \underline{n}	mA = mC·s ⁻¹	($z_{O_2} = 4$)	2.59	nmol O ₂ ·s ⁻¹	2
\underline{n} to \underline{e}	nmol H ⁺ ·s ⁻¹	($z_{H^+} = 1$)	0.09649	mA	3
\underline{n} to \underline{e}	nmol O ₂ ·s ⁻¹	($z_{O_2} = 4$)	0.38594	mA	3

1297 1 At standard temperature and pressure dry (STPD: 0 °C = 273.15 K and 1 atm = 101.325 kPa =
 1298 760 mmHg), the molar volume of an ideal gas, V_m , and V_{m,O_2} is 22.414 and 22.392 L·mol⁻¹,
 1299 respectively. Rounded to three decimal places, both values yield the conversion factor of 0.744.
 1300 For comparison at normal temperature and pressure dry (NTPD: 20 °C), V_{m,O_2} is 24.038 L·mol⁻¹.
 1301 Note that the *SI* standard pressure is 100 kPa.

1302 2 The multiplication factor is $10^6/(z_B \cdot F)$.

1303 3 The multiplication factor is $z_B \cdot F/10^6$.

1304

1305 **Table 7. Conversion of units with preservation of numerical values.**

Name	Frequently used unit	Equivalent unit	Notes
volume-specific flux, J_{V,O_2}	$\text{pmol}\cdot\text{s}^{-1}\cdot\text{mL}^{-1}$	$\text{nmol}\cdot\text{s}^{-1}\cdot\text{L}^{-1}$	1
cell-specific flow, $I_{O_2/\text{cell}}$	$\text{mmol}\cdot\text{s}^{-1}\cdot\text{L}^{-1}$	$\text{mol}\cdot\text{s}^{-1}\cdot\text{m}^{-3}$	
	$\text{pmol}\cdot\text{s}^{-1}\cdot 10^{-6}$ cells	$\text{amol}\cdot\text{s}^{-1}\cdot\text{cell}^{-1}$	2
cell number concentration, C_{Nce}	$\text{pmol}\cdot\text{s}^{-1}\cdot 10^{-9}$ cells	$\text{zmol}\cdot\text{s}^{-1}\cdot\text{cell}^{-1}$	3
	10^6 cells $\cdot\text{mL}^{-1}$	10^9 cells $\cdot\text{L}^{-1}$	
mitochondrial protein concentration, C_{mtE}	0.1 mg $\cdot\text{mL}^{-1}$	0.1 g $\cdot\text{L}^{-1}$	
mass-specific flux, $J_{O_2/m}$	$\text{pmol}\cdot\text{s}^{-1}\cdot\text{mg}^{-1}$	$\text{nmol}\cdot\text{s}^{-1}\cdot\text{g}^{-1}$	4
catabolic power, P_k	$\mu\text{W}\cdot 10^{-6}$ cells	$\text{pW}\cdot\text{cell}^{-1}$	1
volume	1,000 L	m^3 (1,000 kg)	
	L	dm^3 (kg)	
	mL	cm^3 (g)	
	μL	mm^3 (mg)	
	fL	μm^3 (pg)	5
amount of substance concentration	$\text{M} = \text{mol}\cdot\text{L}^{-1}$	$\text{mol}\cdot\text{dm}^{-3}$	

1306 1 pmol: picomole = 10^{-12} mol1307 2 amol: attomole = 10^{-18} mol1308 3 zmol: zeptomole = 10^{-21} mol

1309

1310 Although volume is expressed as m^3 using the *SI* base unit, the litre [dm^3] is a conventional unit
 1311 of volume for concentration and is used for most solution chemical kinetics. If one multiplies $I_{O_2/Nce}$ by
 1312 C_{Nce} , then the result will not only be the amount of O_2 [mol] consumed per time [s^{-1}] in one litre [L^{-1}],
 1313 but also the change in O_2 concentration per second (for any volume of an ideally closed system). This
 1314 is ideal for kinetic modeling as it blends with chemical rate equations where concentrations are typically
 1315 expressed in $\text{mol}\cdot\text{L}^{-1}$ (Wagner *et al.* 2011). In studies of multinuclear cells—such as differentiated
 1316 skeletal muscle cells—it is easy to determine the number of nuclei but not the total number of cells. A
 1317 generalized concept, therefore, is obtained by substituting cells by nuclei as the sample entity. This does
 1318 not hold, however, for enucleated platelets.

1319 For studies of cells, we recommend that respiration be expressed, as far as possible, as: (1) O_2
 1320 flux normalized for a mitochondrial marker, for separation of the effects of mitochondrial quality and
 1321 content on cell respiration (this includes *FCRs* as a normalization for a functional mitochondrial
 1322 marker); (2) O_2 flux in units of cell volume or mass, for comparison of respiration of cells with different
 1323 cell size (Renner *et al.* 2003) and with studies on tissue preparations, and (3) O_2 flow in units of attomole
 1324 (10^{-18} mol) of O_2 consumed in a second by each cell [$\text{amol}\cdot\text{s}^{-1}\cdot\text{cell}^{-1}$], numerically equivalent to
 1325 [$\text{pmol}\cdot\text{s}^{-1}\cdot 10^{-6}$ cells]. This convention allows information to be easily used when designing experiments
 1326 in which O_2 flow must be considered. For example, to estimate the volume-specific O_2 flux in an
 1327 instrument chamber that would be expected at a particular cell number concentration, one simply needs
 1328 to multiply the flow per cell by the number of cells per volume of interest. This provides the amount of
 1329 O_2 [mol] consumed per time [s^{-1}] per unit volume [L^{-1}]. At an O_2 flow of 100 $\text{amol}\cdot\text{s}^{-1}\cdot\text{cell}^{-1}$ and a cell
 1330 density of 10^9 cells $\cdot\text{L}^{-1}$ (10^6 cells $\cdot\text{mL}^{-1}$), the volume-specific O_2 flux is 100 $\text{nmol}\cdot\text{s}^{-1}\cdot\text{L}^{-1}$ (100
 1331 $\text{pmol}\cdot\text{s}^{-1}\cdot\text{mL}^{-1}$).

1332 ET-capacity in human cell types including HEK 293, primary HUVEC and fibroblasts ranges
 1333 from 50 to 180 $\text{amol}\cdot\text{s}^{-1}\cdot\text{cell}^{-1}$, measured in intact cells in the noncoupled state (see Gnaiger 2014). At
 1334 100 $\text{amol}\cdot\text{s}^{-1}\cdot\text{cell}^{-1}$ corrected for *Rox*, the current across the mt-membranes, I_{H+e} , approximates 193
 1335 $\text{pA}\cdot\text{cell}^{-1}$ or 0.2 nA per cell. See Rich (2003) for an extension of quantitative bioenergetics from the
 1336 molecular to the human scale, with a transmembrane proton flux equivalent to 520 A in an adult at a
 1337 catabolic power of -110 W. Modelling approaches illustrate the link between protonmotive force and
 1338 currents (Willis *et al.* 2016).

1339 We consider isolated mitochondria as powerhouses and proton pumps as molecular machines to
 1340 relate experimental results to energy metabolism of the intact cell. The cellular $\text{P}\gg/\text{O}_2$ based on oxidation

of glycogen is increased by the glycolytic (fermentative) substrate-level phosphorylation of 3 P_»/Glyc or 0.5 mol P_» for each mol O₂ consumed in the complete oxidation of a mol glycosyl unit (Glyc). Adding 0.5 to the mitochondrial P_»/O₂ ratio of 5.4 yields a bioenergetic cell physiological P_»/O₂ ratio close to 6. Two NADH equivalents are formed during glycolysis and transported from the cytosol into the mitochondrial matrix, either by the malate-aspartate shuttle or by the glycerophosphate shuttle (**Figure 2A**) resulting in different theoretical yields of ATP generated by mitochondria, the energetic cost of which potentially must be taken into account. Considering also substrate-level phosphorylation in the TCA cycle, this high P_»/O₂ ratio not only reflects proton translocation and OXPHOS studied in isolation, but integrates mitochondrial physiology with energy transformation in the living cell (Gnaiger 1993a).

7. Conclusions

Catabolic cell respiration is the process of exergonic and exothermic energy transformation in which scalar redox reactions are coupled to vectorial ion translocation across a semipermeable membrane, which separates the small volume of a bacterial cell or mitochondrion from the larger volume of its surroundings. The electrochemical exergy can be partially conserved in the phosphorylation of ADP to ATP or in ion pumping, or dissipated in an electrochemical short-circuit. Respiration is thus clearly distinguished from fermentation as the counterpart of cellular core energy metabolism. An O₂ flux balance scheme illustrates the relationships and general definitions (**Figures 1 and 2**).

Box 3: Recommendations for studies with mitochondrial preparations

- Normalization of respiratory rates should be provided as far as possible:
 1. *Biophysical normalization*: on a per cell basis as O₂ flow; this may not be possible when dealing with coenocytic organisms or tissues without cross-walls separating individual cells (e.g., filamentous fungi, muscle fibers)
 2. *Cellular normalization*: per g protein; per cell- or tissue-mass as mass-specific O₂ flux; per cell volume as cell volume-specific flux
 3. *Mitochondrial normalization*: per mitochondrial marker as mt-specific flux.
- With information on cell size and the use of multiple normalizations, maximum potential information is available (Renner *et al.* 2003; Wagner *et al.* 2011; Gnaiger 2014). Reporting flow in a respiratory chamber [nmol·s⁻¹] is discouraged, since it restricts the analysis to intra-experimental comparison of relative (qualitative) differences.
- Catabolic mitochondrial respiration is distinguished from residual O₂ consumption. Fluxes in mitochondrial coupling states should be, as far as possible, corrected for residual O₂ consumption.
- Different mechanisms of uncoupling should be distinguished by defined terms. The tightness of coupling relates to these uncoupling mechanisms, whereas the coupling stoichiometry varies as a function the substrate type involved in ET-pathways with either three or two redox proton pumps operating in series. Separation of tightness of coupling from the pathway-dependent coupling stoichiometry is possible only when the substrate type undergoing oxidation remains the same for respiration in LEAK-, OXPHOS-, and ET-states. In studies of the tightness of coupling, therefore, simple substrate-inhibitor combinations should be applied to exclude a shift in substrate competition which may occur when providing physiological substrate cocktails.
- In studies of isolated mitochondria, the mitochondrial recovery and yield should be reported. Experimental criteria for evaluation of purity versus integrity should be considered. Mitochondrial markers—such as citrate synthase activity as an enzymatic matrix marker—provide a link to the tissue of origin on the basis of calculating the mitochondrial recovery, *i.e.*, the fraction of mitochondrial marker obtained from a unit mass of tissue. Total mitochondrial protein is frequently applied as a mitochondrial marker, which is restricted to isolated mitochondria.
- In studies of permeabilized cells, the viability of the cell culture or cell suspension of origin should be reported. Normalization should be evaluated for total cell count or viable cell count.
- Terms and symbols are summarized in **Table 8**. Their use will facilitate transdisciplinary communication and support further developments towards a consistent theory of bioenergetics and mitochondrial physiology. Technical terms related to and defined with normal words can be used as index terms in databases, support the creation of ontologies towards semantic information processing

1397 (MitoPedia), and help in communicating analytical findings as impactful data-driven stories.
 1398 ‘Making data available without making it understandable may be worse than not making it available
 1399 at all’ (National Academies of Sciences, Engineering, and Medicine 2018). Success will depend on
 1400 taking next steps: (1) exhaustive text-mining considering Omics data and functional data; (2) network
 1401 analysis of Omics data with bioinformatics tools; (3) cross-validation with distinct bioinformatics
 1402 approaches; (4) correlation with functional data; (5) guidelines for biological validation of network
 1403 data. This is a call to carefully contribute to FAIR principles (Findable, Accessible, Interoperable,
 1404 Reusable) for the sharing of scientific data.
 1405

1406
 1407 **Table 8. Terms, symbols, and units.**
 1408

1409	1410	1411	1412	1413
Term	Symbol	Unit	Links and comments	
1413	AOX		Figure 2B	
1414	n_B	[mol]		
1415	Y_{P_{\gg}/O_2}		P \gg /O ₂ ratio measured in any respiratory state	
1417	k		Figure 1 and 3	
1418	J_{kO_2}	<i>varies</i>	Figure 1 and 3	
1419	N_{ce}	[x]	$N_{ce} = N_{vce} + N_{dce}$; Table 5	
1420	J_{rO_2}	<i>varies</i>	Figure 1	
1421	VI		$VI = N_{vce}/N_{ce} = 1 - N_{dce}/N_{ce}$	
1422	z_B		Table 6; $z_{O_2} = 4$	
1423	CI to CIV		respiratory ET Complexes; Figure 2B	
1425	$c_B = n_B \cdot V^{-1}$; [B]	[mol·m ⁻³]	Box 2	
1426	CCS		Section 2.4.1	
1427	N_{dce}	[x]	non-viable cells, loss of plasma membrane barrier function; Table 5	
1429	\underline{e}	[C]	Table 6	
1430	ETS		state; Figure 2B, Figure 4	
1431	I_B	[mol·s ⁻¹]	system-related extensive quantity; Figure 6	
1433	J_B	<i>varies</i>	size-specific quantity; Figure 6	
1434	P _i		Figure 2C	
1435	PiC		Figure 2C	
1437	N_{vce}	[x]	viable cells, intact of plasma membrane barrier function; Table 5	
1439	LEAK		state; Table 1, Figure 4	
1440	\underline{m}	[kg]	Table 4, Figure 6	
1441	m_X	[kg]	Table 4	
1442	m_d	[kg]	mass of sample X; Figure 6 (frequently called dry weight)	
1444	m_w	[kg]	mass of sample X; Figure 6 (frequently called wet weight)	
1446	$M_X = m_X \cdot N_X^{-1}$	[kg·x ⁻¹]	mass of entity X; Table 4	
1447	MITOCARTA		https://www.broadinstitute.org/scientific-community/science/programs/metabolic-disease-program/publications/mitocarta/mitocarta-in-0	

1452	MitoPedia			http://www.bioblast.at/index.php/MitoPedia
1453	mitochondria or mitochondrial	mt		Box 1
1454	mitochondrial DNA	mtDNA		Box 1
1455	mitochondrial concentration	$C_{mtE} = mtE \cdot V^{-1}$	[mtEU·m ⁻³]	Table 4
1456	mitochondrial content	mtE_X	[mtEU·x ⁻¹]	$mtE_X = mtE \cdot N_X^{-1}$; Table 4
1457	mitochondrial			
1458	elementary component	mtE	[mtEU]	quantity of mt-marker; Table 4
1459	mitochondrial elementary unit	mtEU	<i>varies</i>	specific units for mt-marker; Table 4
1460	mitochondrial inner membrane	mtIM		MIM is widely used; the first M is replaced by mt; Figure 2; Box 1
1461				
1462	mitochondrial outer membrane	mtOM		MOM is widely used; the first M is replaced by mt; Figure 2; Box 1
1463				
1464	mitochondrial recovery	Y_{mtE}		fraction of mtE recovered in sample from the tissue of origin
1465				
1466	mitochondrial yield	$Y_{mtE/m}$		mt-yield per tissues mass; $Y_{mtE/m} = Y_{mtE} \cdot D_{mtE}$
1467				
1468	molar format	\underline{n}	[mol]	Table 6
1469	negative	neg		Figure 4
1470	number concentration of X	C_{NX}	[x·m ⁻³]	Table 4
1471	number format	\underline{N}	[x]	Table 4, Figure 6
1472	number of entities X	N_X	[x]	Table 4, Figure 6
1473	number of entity B	N_B	[x]	Table 4
1474	oxidative phosphorylation	OXPPOS		state; Table 1, Figure 4
1475	oxygen concentration	$c_{O_2} = n_{O_2} \cdot V^{-1}$	[mol·m ⁻³]	[O ₂]; Section 3.2
1476	oxygen flux, in reaction r	J_{rO_2}	<i>varies</i>	Figure 1
1477	pathway control state	PCS		Section 2.2
1478	permeabilized cell number	N_{pce}	[x]	experimental permeabilization of plasma membrane; Table 5
1479				
1480	phosphorylation of ADP to ATP	P»		Section 2.2
1481	P»/O ₂ ratio	P»/O ₂		mechanistic $Y_{P»/O_2}$, calculated from pump stoichiometries; Figure 2B
1482				
1483	positive	pos		Figure 4
1484	proton in the negative compartment	H ⁺ _{neg}		Figure 4
1485	proton in the positive compartment	H ⁺ _{pos}		Figure 4
1486	protonmotive force	pmf	[V]	Figures 1, 2A and 4; Table 1
1487	rate of electron transfer in ET state	E		ET-capacity; Table 1
1488	rate of LEAK respiration	L		Table 1
1489	rate of oxidative phosphorylation	P		OXPPOS capacity; Table 1
1490	rate of residual oxygen consumption	Ro_x		Table 1, Figure 1
1491	residual oxygen consumption	ROX		state; Table 1
1492	respiratory supercomplex	SC I _n III _n IV _n		supramolecular assemblies composed of variable copy numbers (n) of CI, CIII and CIV; Box 1
1493				
1494				
1495	specific mitochondrial density	$D_{mtE} = mtE \cdot m_X^{-1}$	[mtEU·kg ⁻¹]	Table 4
1496	substrate-uncoupler-inhibitor-titration protocol	SUIT		##
1497				
1498	volume	V	[m ⁻³]	Table 7
1499	volume format	\underline{V}	[m ⁻³]	Table 6

1501
 1502 Experimentally, respiration is separated in mitochondrial preparations from the interactions with
 1503 the fermentative pathways of the intact cell. OXPPOS analysis is based on the study of mitochondrial
 1504 preparations complementary to bioenergetic investigations of intact cells and organisms—from model
 1505 organisms to the human species including healthy and diseased persons (patients). Different mechanisms
 1506 of respiratory uncoupling have to be distinguished (**Figure 3**). Metabolic fluxes measured in defined

1507 coupling and pathway control states (**Figures 5 and 6**) provide insights into the meaning of cellular and
1508 organismic respiration.

1509 The optimal choice for expressing mitochondrial and cell respiration as O₂ flow per biological
1510 sample, and normalization for specific tissue-markers (volume, mass, protein) and mitochondrial
1511 markers (volume, protein, content, mtDNA, activity of marker enzymes, respiratory reference state) is
1512 guided by the scientific question under study. Interpretation of the data depends critically on appropriate
1513 normalization (**Figure 6**).

1514 MitoEAGLE can serve as a gateway to better diagnose mitochondrial respiratory adaptations and
1515 defects linked to genetic variation, age-related health risks, sex-specific mitochondrial performance,
1516 lifestyle with its effects on degenerative diseases, and thermal and chemical environment. The present
1517 recommendations on coupling control states and rates, linked to the concept of the protonmotive force,
1518 are focused on studies with mitochondrial preparations (**Box 3**). These will be extended in a series of
1519 reports on pathway control of mitochondrial respiration, respiratory states in intact cells, and
1520 harmonization of experimental procedures.

1521 **Acknowledgements**

1522 We thank M. Beno for management assistance. This publication is based upon work from COST Action
1523 CA15203 MitoEAGLE, supported by COST (European Cooperation in Science and Technology), and
1524 K-Regio project MitoFit (E.G.).

1525
1526

1527 **Competing financial interests:** E.G. is founder and CEO of Oroboros Instruments, Innsbruck, Austria.

1528

1529 **References**

- 1530
1531 Altmann R (1894) Die Elementarorganismen und ihre Beziehungen zu den Zellen. Zweite vermehrte Auflage.
1532 Verlag Von Veit & Comp, Leipzig:160 pp.
- 1533 Baggeto LG, Testa-Perussini R (1990) Role of acetoin on the regulation of intermediate metabolism of Ehrlich
1534 ascites tumor mitochondria: its contribution to membrane cholesterol enrichment modifying passive proton
1535 permeability. Arch Biochem Biophys 283:341-8.
- 1536 Beard DA (2005) A biophysical model of the mitochondrial respiratory system and oxidative phosphorylation.
1537 PLoS Comput Biol 1(4):e36.
- 1538 Benda C (1898) Weitere Mitteilungen über die Mitochondria. Verh Dtsch Physiol Ges:376-83.
- 1539 Birkedal R, Laasmaa M, Vendelin M (2014) The location of energetic compartments affects energetic
1540 communication in cardiomyocytes. Front Physiol 5:376.
- 1541 Blier PU, Dufresne F, Burton RS (2001) Natural selection and the evolution of mtDNA-encoded peptides:
1542 evidence for intergenomic co-adaptation. Trends Genet 17:400-6.
- 1543 Blier PU, Guderley HE (1993) Mitochondrial activity in rainbow trout red muscle: the effect of temperature on
1544 the ADP-dependence of ATP synthesis. J Exp Biol 176:145-58.
- 1545 Breton S, Beaupré HD, Stewart DT, Hoeh WR, Blier PU (2007) The unusual system of doubly uniparental
1546 inheritance of mtDNA: isn't one enough? Trends Genet 23:465-74.
- 1547 Brown GC (1992) Control of respiration and ATP synthesis in mammalian mitochondria and cells. Biochem J
1548 284:1-13.
- 1549 Burger G, Gray MW, Forget L, Lang BF (2013) Strikingly bacteria-like and gene-rich mitochondrial genomes
1550 throughout jakobid protists. Genome Biol Evol 5:418-38.
- 1551 Calvo SE, Klauser CR, Mootha VK (2016) MitoCarta2.0: an updated inventory of mammalian mitochondrial
1552 proteins. Nucleic Acids Research 44:D1251-7.
- 1553 Calvo SE, Julien O, Clauser KR, Shen H, Kamer KJ, Wells JA, Mootha VK (2017) Comparative analysis of
1554 mitochondrial N-termini from mouse, human, and yeast. Mol Cell Proteomics 16:512-23.
- 1555 Campos JC, Queliconi BB, Bozi LHM, Bechara LRG, Dourado PMM, Andres AM, Jannig PR, Gomes KMS,
1556 Zambelli VO, Rocha-Resende C, Guatimosim S, Brum PC, Mochly-Rosen D, Gottlieb RA, Kowaltowski AJ,
1557 Ferreira JCB (2017) Exercise reestablishes autophagic flux and mitochondrial quality control in heart failure.
1558 Autophagy 13:1304-317.
- 1559 Canton M, Luvisetto S, Schmehl I, Azzone GF (1995) The nature of mitochondrial respiration and
1560 discrimination between membrane and pump properties. Biochem J 310:477-81.
- 1561 Carrico C, Meyer JG, He W, Gibson BW, Verdin E (2018) The mitochondrial acylome emerges: proteomics,
1562 regulation by Sirtuins, and metabolic and disease implications. Cell Metab 27:497-512.
- 1563 Chan DC (2006) Mitochondria: dynamic organelles in disease, aging, and development. Cell 125:1241-52.
- 1564 Chance B, Williams GR (1955a) Respiratory enzymes in oxidative phosphorylation. I. Kinetics of oxygen
1565 utilization. J Biol Chem 217:383-93.

- 1566 Chance B, Williams GR (1955b) Respiratory enzymes in oxidative phosphorylation: III. The steady state. *J Biol*
 1567 *Chem* 217:409-27.
- 1568 Chance B, Williams GR (1955c) Respiratory enzymes in oxidative phosphorylation. IV. The respiratory chain. *J*
 1569 *Biol Chem* 217:429-38.
- 1570 Chance B, Williams GR (1956) The respiratory chain and oxidative phosphorylation. *Adv Enzymol Relat Subj*
 1571 *Biochem* 17:65-134.
- 1572 Chowdhury SK, Djordjevic J, Albensi B, Fernyhough P (2015) Simultaneous evaluation of substrate-dependent
 1573 oxygen consumption rates and mitochondrial membrane potential by TMRM and safranin in cortical
 1574 mitochondria. *Biosci Rep* 36:e00286.
- 1575 Cobb LJ, Lee C, Xiao J, Yen K, Wong RG, Nakamura HK, Mehta HH, Gao Q, Ashur C, Huffman DM, Wan J,
 1576 Muzumdar R, Barzilai N, Cohen P (2016) Naturally occurring mitochondrial-derived peptides are age-
 1577 dependent regulators of apoptosis, insulin sensitivity, and inflammatory markers. *Aging (Albany NY)* 8:796-
 1578 809.
- 1579 Cohen ER, Cvitas T, Frey JG, Holmström B, Kuchitsu K, Marquardt R, Mills I, Pavese F, Quack M, Stohner J,
 1580 Strauss HL, Takami M, Thor HL (2008) Quantities, units and symbols in physical chemistry, IUPAC Green
 1581 Book, 3rd Edition, 2nd Printing, IUPAC & RSC Publishing, Cambridge.
- 1582 Cooper H, Hedges LV, Valentine JC, eds (2009) The handbook of research synthesis and meta-analysis. Russell
 1583 Sage Foundation.
- 1584 Coopersmith J (2010) Energy, the subtle concept. The discovery of Feynman's blocks from Leibnitz to Einstein.
 1585 Oxford University Press:400 pp.
- 1586 Cummins J (1998) Mitochondrial DNA in mammalian reproduction. *Rev Reprod* 3:172-82.
- 1587 Dai Q, Shah AA, Garde RV, Yonish BA, Zhang L, Medvitz NA, Miller SE, Hansen EL, Dunn CN, Price TM
 1588 (2013) A truncated progesterone receptor (PR-M) localizes to the mitochondrion and controls cellular
 1589 respiration. *Mol Endocrinol* 27:741-53.
- 1590 Daum B, Walter A, Horst A, Osiewacz HD, Kühlbrandt W (2013) Age-dependent dissociation of ATP synthase
 1591 dimers and loss of inner-membrane cristae in mitochondria. *Proc Natl Acad Sci U S A* 110:15301-6.
- 1592 Divakaruni AS, Brand MD (2011) The regulation and physiology of mitochondrial proton leak. *Physiology*
 1593 (Bethesda) 26:192-205.
- 1594 Doerrier C, Garcia-Souza LF, Krumschnabel G, Wohlfarter Y, Mészáros AT, Gnaiger E (2018) High-Resolution
 1595 FluoRespirometry and OXPHOS protocols for human cells, permeabilized fibres from small biopsies of
 1596 muscle, and isolated mitochondria. *Methods Mol Biol* 1782 (Palmeira CM, Moreno AJ, eds): Mitochondrial
 1597 Bioenergetics, 978-1-4939-7830-4.
- 1598 Doskey CM, van 't Erve TJ, Wagner BA, Buettner GR (2015) Moles of a substance per cell is a highly
 1599 informative dosing metric in cell culture. *PLOS ONE* 10:e0132572.
- 1600 Drahota Z, Milerová M, Stieglerová A, Houstek J, Ostádal B (2004) Developmental changes of cytochrome *c*
 1601 oxidase and citrate synthase in rat heart homogenate. *Physiol Res* 53:119-22.
- 1602 Duarte FV, Palmeira CM, Rolo AP (2014) The role of microRNAs in mitochondria: small players acting wide.
 1603 *Genes (Basel)* 5:865-86.
- 1604 Ehinger JK, Morota S, Hansson MJ, Paul G, Elmér E (2015) Mitochondrial dysfunction in blood cells from
 1605 amyotrophic lateral sclerosis patients. *J Neurol* 262:1493-503.
- 1606 Ernster L, Schatz G (1981) Mitochondria: a historical review. *J Cell Biol* 91:227s-55s.
- 1607 Estabrook RW (1967) Mitochondrial respiratory control and the polarographic measurement of ADP:O ratios.
 1608 *Methods Enzymol* 10:41-7.
- 1609 Faber C, Zhu ZJ, Castellino S, Wagner DS, Brown RH, Peterson RA, Gates L, Barton J, Bickett M, Hagerty L,
 1610 Kimbrough C, Sola M, Bailey D, Jordan H, Elangbam CS (2014) Cardiolipin profiles as a potential
 1611 biomarker of mitochondrial health in diet-induced obese mice subjected to exercise, diet-restriction and
 1612 ephedrine treatment. *J Appl Toxicol* 34:1122-9.
- 1613 Feagin JE, Harrell MI, Lee JC, Coe KJ, Sands BH, Cannone JJ, Tami G, Schnare MN, Gutell RR (2012) The
 1614 fragmented mitochondrial ribosomal RNAs of *Plasmodium falciparum*. *PLoS One* 7:e38320.
- 1615 Fell D (1997) Understanding the control of metabolism. Portland Press.
- 1616 Forstner H, Gnaiger E (1983) Calculation of equilibrium oxygen concentration. In: Polarographic Oxygen
 1617 Sensors. Aquatic and Physiological Applications. Gnaiger E, Forstner H (eds), Springer, Berlin, Heidelberg,
 1618 New York:321-33.
- 1619 Garlid KD, Beavis AD, Ratkje SK (1989) On the nature of ion leaks in energy-transducing membranes. *Biochim*
 1620 *Biophys Acta* 976:109-20.
- 1621 Garlid KD, Semrad C, Zinchenko V. Does redox slip contribute significantly to mitochondrial respiration? In:
 1622 Schuster S, Rigoulet M, Ouhabi R, Mazat J-P, eds (1993) Modern trends in biothermokinetics. Plenum Press,
 1623 New York, London:287-93.
- 1624 Gerö D, Szabo C (2016) Glucocorticoids suppress mitochondrial oxidant production via upregulation of
 1625 uncoupling protein 2 in hyperglycemic endothelial cells. *PLoS One* 11:e0154813.

- 1626 Gnaiger E. Efficiency and power strategies under hypoxia. Is low efficiency at high glycolytic ATP production a
 1627 paradox? In: *Surviving Hypoxia: Mechanisms of Control and Adaptation*. Hochachka PW, Lutz PL, Sick T,
 1628 Rosenthal M, Van den Thillart G, eds (1993a) CRC Press, Boca Raton, Ann Arbor, London, Tokyo:77-109.
 1629 Gnaiger E (1993b) Nonequilibrium thermodynamics of energy transformations. *Pure Appl Chem* 65:1983-2002.
 1630 Gnaiger E (2001) Bioenergetics at low oxygen: dependence of respiration and phosphorylation on oxygen and
 1631 adenosine diphosphate supply. *Respir Physiol* 128:277-97.
 1632 Gnaiger E (2009) Capacity of oxidative phosphorylation in human skeletal muscle. *New perspectives of*
 1633 *mitochondrial physiology*. *Int J Biochem Cell Biol* 41:1837-45.
 1634 Gnaiger E (2014) *Mitochondrial pathways and respiratory control. An introduction to OXPHOS analysis*. 4th ed.
 1635 *Mitochondr Physiol Network* 19.12. Oroboros MiPNet Publications, Innsbruck:80 pp.
 1636 Gnaiger E, Méndez G, Hand SC (2000) High phosphorylation efficiency and depression of uncoupled respiration
 1637 in mitochondria under hypoxia. *Proc Natl Acad Sci USA* 97:11080-5.
 1638 Greggio C, Jha P, Kulkarni SS, Lagarrigue S, Brosky NT, Boutant M, Wang X, Conde Alonso S, Ofori E,
 1639 Auwerx J, Cantó C, Amati F (2017) Enhanced respiratory chain supercomplex formation in response to
 1640 exercise in human skeletal muscle. *Cell Metab* 25:301-11.
 1641 Hinkle PC (2005) P/O ratios of mitochondrial oxidative phosphorylation. *Biochim Biophys Acta* 1706:1-11.
 1642 Hofstadter DR (1979) Gödel, Escher, Bach: An eternal golden braid. A metaphorical fugue on minds and
 1643 machines in the spirit of Lewis Carroll. Harvester Press:499 pp.
 1644 Illaste A, Laasmaa M, Peterson P, Vendelin M (2012) Analysis of molecular movement reveals latticelike
 1645 obstructions to diffusion in heart muscle cells. *Biophys J* 102:739-48.
 1646 Jasienski M, Bazzaz FA (1999) The fallacy of ratios and the testability of models in biology. *Oikos* 84:321-26.
 1647 Jepihhina N, Beraud N, Sepp M, Birkedal R, Vendelin M (2011) Permeabilized rat cardiomyocyte response
 1648 demonstrates intracellular origin of diffusion obstacles. *Biophys J* 101:2112-21.
 1649 Karnkowska A, Vacek V, Zubáčová Z, Treitli SC, Petrželková R, Eme L, Novák L, Žárský V, Barlow LD,
 1650 Herman EK, Soukal P, Hroudová M, Doležal P, Stairs CW, Roger AJ, Eliáš M, Dacks JB, Vlček Č, Hampl V
 1651 (2016) A eukaryote without a mitochondrial organelle. *Curr Biol* 26:1274-84.
 1652 Klepinin A, Ounpuu L, Guzun R, Chekulayev V, Timohhina N, Tepp K, Shevchuk I, Schlattner U, Kaambre T
 1653 (2016) Simple oxygraphic analysis for the presence of adenylate kinase 1 and 2 in normal and tumor cells. *J*
 1654 *Bioenerg Biomembr* 48:531-48.
 1655 Klingenberg M (2017) UCP1 - A sophisticated energy valve. *Biochimie* 134:19-27.
 1656 Koit A, Shevchuk I, Ounpuu L, Klepinin A, Chekulayev V, Timohhina N, Tepp K, Puurand M, Truu L, Heck K,
 1657 Valvere V, Guzun R, Kaambre T (2017) Mitochondrial respiration in human colorectal and breast cancer
 1658 clinical material is regulated differently. *Oxid Med Cell Longev* 1372640.
 1659 Komlódi T, Tretter L (2017) Methylene blue stimulates substrate-level phosphorylation catalysed by succinyl-
 1660 CoA ligase in the citric acid cycle. *Neuropharmacology* 123:287-98.
 1661 Korn E (1969) Cell membranes: structure and synthesis. *Annu Rev Biochem* 38:263-88.
 1662 Lai N, M Kummitha C, Rosca MG, Fujioka H, Tandler B, Hoppel CL (2018) Isolation of mitochondrial
 1663 subpopulations from skeletal muscle: optimizing recovery and preserving integrity. *Acta Physiol*
 1664 (Oxf):e13182. doi: 10.1111/apha.13182.
 1665 Lane N (2005) *Power, sex, suicide: mitochondria and the meaning of life*. Oxford University Press:354 pp.
 1666 Larsen S, Nielsen J, Neigaard Nielsen C, Nielsen LB, Wibrand F, Stride N, Schroder HD, Boushel RC, Helge
 1667 JW, Dela F, Hey-Mogensen M (2012) Biomarkers of mitochondrial content in skeletal muscle of healthy
 1668 young human subjects. *J Physiol* 590:3349-60.
 1669 Lee C, Zeng J, Drew BG, Sallam T, Martin-Montalvo A, Wan J, Kim SJ, Mehta H, Hevener AL, de Cabo R,
 1670 Cohen P (2015) The mitochondrial-derived peptide MOTS-c promotes metabolic homeostasis and reduces
 1671 obesity and insulin resistance. *Cell Metab* 21:443-54.
 1672 Lee SR, Kim HK, Song IS, Youm J, Dizon LA, Jeong SH, Ko TH, Heo HJ, Ko KS, Rhee BD, Kim N, Han J
 1673 (2013) Glucocorticoids and their receptors: insights into specific roles in mitochondria. *Prog Biophys Mol*
 1674 *Biol* 112:44-54.
 1675 Leek BT, Mudaliar SR, Henry R, Mathieu-Costello O, Richardson RS (2001) Effect of acute exercise on citrate
 1676 synthase activity in untrained and trained human skeletal muscle. *Am J Physiol Regul Integr Comp Physiol*
 1677 280:R441-7.
 1678 Lemieux H, Blier PU, Gnaiger E (2017) Remodeling pathway control of mitochondrial respiratory capacity by
 1679 temperature in mouse heart: electron flow through the Q-junction in permeabilized fibers. *Sci Rep* 7:2840.
 1680 Lenaz G, Tioli G, Falasca AI, Genova ML (2017) Respiratory supercomplexes in mitochondria. In: *Mechanisms*
 1681 *of primary energy transduction in biology*. M Wikstrom (ed) Royal Society of Chemistry Publishing, London,
 1682 UK:296-337.
 1683 Liu S, Roellig DM, Guo Y, Li N, Frace MA, Tang K, Zhang L, Feng Y, Xiao L (2016) Evolution of mitosome
 1684 metabolism and invasion-related proteins in *Cryptosporidium*. *BMC Genomics* 17:1006.
 1685 Margulis L (1970) *Origin of eukaryotic cells*. New Haven: Yale University Press.
 1686 Meinild Lundby AK, Jacobs RA, Gehrig S, de Leur J, Hauser M, Bonne TC, Flück D, Dandanell S, Kirk N,
 1687 Kaech A, Ziegler U, Larsen S, Lundby C (2018) Exercise training increases skeletal muscle mitochondrial

- 1688 volume density by enlargement of existing mitochondria and not de novo biogenesis. *Acta Physiol* 222,
1689 e12905.
- 1690 Menshikova EV, Ritov VB, Fairfull L, Ferrell RE, Kelley DE, Goodpaster BH (2006) Effects of exercise on
1691 mitochondrial content and function in aging human skeletal muscle. *J Gerontol A Biol Sci Med Sci* 61:534-
1692 40.
- 1693 Menshikova EV, Ritov VB, Ferrell RE, Azuma K, Goodpaster BH, Kelley DE (2007) Characteristics of skeletal
1694 muscle mitochondrial biogenesis induced by moderate-intensity exercise and weight loss in obesity. *J Appl*
1695 *Physiol* (1985) 103:21-7.
- 1696 Menshikova EV, Ritov VB, Toledo FG, Ferrell RE, Goodpaster BH, Kelley DE (2005) Effects of weight loss
1697 and physical activity on skeletal muscle mitochondrial function in obesity. *Am J Physiol Endocrinol Metab*
1698 288:E818-25.
- 1699 Miller GA (1991) *The science of words*. Scientific American Library New York:276 pp.
- 1700 Mitchell P (1961) Coupling of phosphorylation to electron and hydrogen transfer by a chemi-osmotic type of
1701 mechanism. *Nature* 191:144-8.
- 1702 Mitchell P (2011) Chemiosmotic coupling in oxidative and photosynthetic phosphorylation. *Biochim Biophys*
1703 *Acta Bioenergetics* 1807:1507-38.
- 1704 Mogensen M, Sahlin K, Fernström M, Glintborg D, Vind BF, Beck-Nielsen H, Højlund K (2007) Mitochondrial
1705 respiration is decreased in skeletal muscle of patients with type 2 diabetes. *Diabetes* 56:1592-9.
- 1706 Mohr PJ, Phillips WD (2015) Dimensionless units in the SI. *Metrologia* 52:40-7.
- 1707 Moreno M, Giacco A, Di Munno C, Goglia F (2017) Direct and rapid effects of 3,5-diiodo-L-thyronine (T2).
1708 *Mol Cell Endocrinol* 7207:30092-8.
- 1709 Morrow RM, Picard M, Derbeneva O, Leipzig J, McManus MJ, Gousspillou G, Barbat-Artigas S, Dos Santos C,
1710 Hepple RT, Murdock DG, Wallace DC (2017) Mitochondrial energy deficiency leads to hyperproliferation of
1711 skeletal muscle mitochondria and enhanced insulin sensitivity. *Proc Natl Acad Sci U S A* 114:2705-10.
- 1712 Murley A, Nunnari J (2016) The emerging network of mitochondria-organelle contacts. *Mol Cell* 61:648-53.
- 1713 National Academies of Sciences, Engineering, and Medicine (2018) International coordination for science data
1714 infrastructure: Proceedings of a workshop—in brief. Washington, DC: The National Academies Press. doi:
1715 <https://doi.org/10.17226/25015>.
- 1716 Oemer G, Lackner L, Muigg K, Krumschnabel G, Watschinger K, Sailer S, Lindner H, Gnaiger E, Wortmann
1717 SB, Werner ER, Zschocke J, Keller MA (2018) The molecular structural diversity of mitochondrial
1718 cardiolipins. *Proc Natl Acad Sci U S A* 115:4158-63.
- 1719 Palmfeldt J, Bross P (2017) Proteomics of human mitochondria. *Mitochondrion* 33:2-14.
- 1720 Paradies G, Paradies V, De Benedictis V, Ruggiero FM, Petrosillo G (2014) Functional role of cardiolipin in
1721 mitochondrial bioenergetics. *Biochim Biophys Acta* 1837:408-17.
- 1722 Pesta D, Gnaiger E (2012) High-Resolution Respirometry. OXPHOS protocols for human cells and
1723 permeabilized fibres from small biopsies of human muscle. *Methods Mol Biol* 810:25-58.
- 1724 Pesta D, Hoppel F, Macek C, Messner H, Faulhaber M, Kobel C, Parson W, Burtscher M, Schocke M, Gnaiger
1725 E (2011) Similar qualitative and quantitative changes of mitochondrial respiration following strength and
1726 endurance training in normoxia and hypoxia in sedentary humans. *Am J Physiol Regul Integr Comp Physiol*
1727 301:R1078-87.
- 1728 Price TM, Dai Q (2015) The role of a mitochondrial progesterone receptor (PR-M) in progesterone action.
1729 *Semin Reprod Med* 33:185-94.
- 1730 Puchowicz MA, Varnes ME, Cohen BH, Friedman NR, Kerr DS, Hoppel CL (2004) Oxidative phosphorylation
1731 analysis: assessing the integrated functional activity of human skeletal muscle mitochondria – case studies.
1732 *Mitochondrion* 4:377-85. Puntchart A, Claassen H, Jostarndt K, Hoppeler H, Billeter R (1995) mRNAs of
1733 enzymes involved in energy metabolism and mtDNA are increased in endurance-trained athletes. *Am J*
1734 *Physiol* 269:C619-25.
- 1735 Quiros PM, Mottis A, Auwerx J (2016) Mitonuclear communication in homeostasis and stress. *Nat Rev Mol*
1736 *Cell Biol* 17:213-26.
- 1737 Rackham O, Mercer TR, Filipovska A (2012) The human mitochondrial transcriptome and the RNA-binding
1738 proteins that regulate its expression. *WIREs RNA* 3:675-95.
- 1739 Reichmann H, Hoppeler H, Mathieu-Costello O, von Bergen F, Pette D (1985) Biochemical and ultrastructural
1740 changes of skeletal muscle mitochondria after chronic electrical stimulation in rabbits. *Pflugers Arch* 404:1-
1741 9.
- 1742 Renner K, Amberger A, Konwalinka G, Gnaiger E (2003) Changes of mitochondrial respiration, mitochondrial
1743 content and cell size after induction of apoptosis in leukemia cells. *Biochim Biophys Acta* 1642:115-23.
- 1744 Rice DW, Alverson AJ, Richardson AO, Young GJ, Sanchez-Puerta MV, Munzinger J, Barry K, Boore JL,
1745 Zhang Y, dePamphilis CW, Knox EB, Palmer JD (2016) Horizontal transfer of entire genomes via
1746 mitochondrial fusion in the angiosperm *Amborella*. *Science* 342:1468-73.
- 1747 Rich P (2003) Chemiosmotic coupling: The cost of living. *Nature* 421:583.
- 1748 Rich PR (2013) Chemiosmotic theory. *Encyclopedia Biol Chem* 1:467-72.

- 1749 Roger JA, Munoz-Gomes SA, Kamikawa R (2017) The origin and diversification of mitochondria. *Curr Biol*
 1750 27:R1177-92.
- 1751 Rostovtseva TK, Sheldon KL, Hassanzadeh E, Monge C, Saks V, Bezrukov SM, Sackett DL (2008) Tubulin
 1752 binding blocks mitochondrial voltage-dependent anion channel and regulates respiration. *Proc Natl Acad Sci*
 1753 USA 105:18746-51.
- 1754 Rustin P, Parfait B, Chretien D, Bourgeron T, Djouadi F, Bastin J, Rötig A, Munnich A (1996) Fluxes of
 1755 nicotinamide adenine dinucleotides through mitochondrial membranes in human cultured cells. *J Biol Chem*
 1756 271:14785-90.
- 1757 Saks VA, Veksler VI, Kuznetsov AV, Kay L, Sikk P, Tiivel T, Tranqui L, Olivares J, Winkler K, Wiedemann F,
 1758 Kunz WS (1998) Permeabilised cell and skinned fiber techniques in studies of mitochondrial function in
 1759 vivo. *Mol Cell Biochem* 184:81-100.
- 1760 Salabei JK, Gibb AA, Hill BG (2014) Comprehensive measurement of respiratory activity in permeabilized cells
 1761 using extracellular flux analysis. *Nat Protoc* 9:421-38.
- 1762 Sazanov LA (2015) A giant molecular proton pump: structure and mechanism of respiratory complex I. *Nat Rev*
 1763 Mol Cell Biol 16:375-88.
- 1764 Schneider TD (2006) Claude Shannon: biologist. The founder of information theory used biology to formulate
 1765 the channel capacity. *IEEE Eng Med Biol Mag* 25:30-3.
- 1766 Schönfeld P, Dymkowska D, Wojtczak L (2009) Acyl-CoA-induced generation of reactive oxygen species in
 1767 mitochondrial preparations is due to the presence of peroxisomes. *Free Radic Biol Med* 47:503-9.
- 1768 Schultz J, Wiesner RJ (2000) Proliferation of mitochondria in chronically stimulated rabbit skeletal muscle--
 1769 transcription of mitochondrial genes and copy number of mitochondrial DNA. *J Bioenerg Biomembr* 32:627-
 1770 34.
- 1771 Speijer D (2016) Being right on Q: shaping eukaryotic evolution. *Biochem J* 473:4103-27.
- 1772 Sugiura A, Mattie S, Prudent J, McBride HM (2017) Newly born peroxisomes are a hybrid of mitochondrial and
 1773 ER-derived pre-peroxisomes. *Nature* 542:251-4.
- 1774 Simson P, Jephthina N, Laasmaa M, Peterson P, Birkedal R, Vendelin M (2016) Restricted ADP movement in
 1775 cardiomyocytes: Cytosolic diffusion obstacles are complemented with a small number of open mitochondrial
 1776 voltage-dependent anion channels. *J Mol Cell Cardiol* 97:197-203.
- 1777 Stucki JW, Ineichen EA (1974) Energy dissipation by calcium recycling and the efficiency of calcium transport
 1778 in rat-liver mitochondria. *Eur J Biochem* 48:365-75.
- 1779 Tonkonogi M, Harris B, Sahlin K (1997) Increased activity of citrate synthase in human skeletal muscle after a
 1780 single bout of prolonged exercise. *Acta Physiol Scand* 161:435-6.
- 1781 Torralba D, Baixauli F, Sánchez-Madrid F (2016) Mitochondria know no boundaries: mechanisms and functions
 1782 of intercellular mitochondrial transfer. *Front Cell Dev Biol* 4:107. eCollection 2016.
- 1783 Vamecq J, Schepers L, Parmentier G, Mannaerts GP (1987) Inhibition of peroxisomal fatty acyl-CoA oxidase by
 1784 antimycin A. *Biochem J* 248:603-7.
- 1785 Waczulikova I, Habodaszova D, Cagalinec M, Ferko M, Ulicna O, Mateasik A, Sikurova L, Ziegelhöffer A
 1786 (2007) Mitochondrial membrane fluidity, potential, and calcium transients in the myocardium from acute
 1787 diabetic rats. *Can J Physiol Pharmacol* 85:372-81.
- 1788 Wagner BA, Venkataraman S, Buettner GR (2011) The rate of oxygen utilization by cells. *Free Radic Biol Med*
 1789 51:700-712.
- 1790 Wang H, Hiatt WR, Barstow TJ, Brass EP (1999) Relationships between muscle mitochondrial DNA content,
 1791 mitochondrial enzyme activity and oxidative capacity in man: alterations with disease. *Eur J Appl Physiol*
 1792 Occup Physiol 80:22-7.
- 1793 Watt IN, Montgomery MG, Runswick MJ, Leslie AG, Walker JE (2010) Bioenergetic cost of making an
 1794 adenosine triphosphate molecule in animal mitochondria. *Proc Natl Acad Sci U S A* 107:16823-7.
- 1795 Weibel ER, Hoppeler H (2005) Exercise-induced maximal metabolic rate scales with muscle aerobic capacity. *J*
 1796 *Exp Biol* 208:1635-44.
- 1797 White DJ, Wolff JN, Pierson M, Gemmell NJ (2008) Revealing the hidden complexities of mtDNA inheritance.
 1798 *Mol Ecol* 17:4925-42.
- 1799 Wikström M, Hummer G (2012) Stoichiometry of proton translocation by respiratory complex I and its
 1800 mechanistic implications. *Proc Natl Acad Sci U S A* 109:4431-6.
- 1801 Williams EG, Wu Y, Jha P, Dubuis S, Blattmann P, Argmann CA, Houten SM, Amariuta T, Wolski W,
 1802 Zamboni N, Aebersold R, Auwerx J (2016) Systems proteomics of liver mitochondria function. *Science* 352
 1803 (6291):aad0189
- 1804 Willis WT, Jackman MR, Messer JI, Kuzmiak-Glancy S, Glancy B (2016) A simple hydraulic analog model of
 1805 oxidative phosphorylation. *Med Sci Sports Exerc* 48:990-1000.
- 1806 Ziková A, Hampl V, Paris Z, Týč J, Lukeš J (2016) Aerobic mitochondria of parasitic protists: diverse genomes
 1807 and complex functions. *Mol Biochem Parasitol* 209:46-57.
- 1808
- 1809

1810 Supplement

1811

1812 S1. Manuscript phases and versions - an open-access approach

1813

1814 This manuscript on ‘Mitochondrial respiratory states and rates’ is a position statement in the frame of COST Action
1815 CA15203 MitoEAGLE. The list of co-authors evolved beyond phase 1 in the bottom-up spirit of COST.

1816 The global MitoEAGLE network made it possible to collaborate with a large number of co-authors to reach
1817 consensus on the present manuscript. Nevertheless, we do not consider scientific progress to be supported by
1818 ‘declaration’ statements (other than on ethical or political issues). Our manuscript aims at providing arguments for
1819 further debate rather than pushing opinions. We hope to initiate a much broader process of discussion and want to
1820 raise the awareness on the importance of a consistent terminology for reporting of scientific data in the field of
1821 bioenergetics, mitochondrial physiology and pathology. Quality of research requires quality of communication.
1822 Some established researchers in the field may not want to re-consider the use of jargon which has become
1823 established despite deficiencies of accuracy and meaning. In the long run, superior standards will become accepted.
1824 We hope to contribute to this evolutionary process, with an emphasis on harmonization rather than standardization.

1825 *Phase 1* The protonmotive force and respiratory control

1826 http://www.mitoeagle.org/index.php/The_protonmotive_force_and_respiratory_control

1827 • 2017-04-09 to 2017-09-18 (44 versions)

1828 • 2017-09-21 to 2018-02-06 (44+21 versions)

1829 http://www.mitoeagle.org/index.php/MitoEAGLE_preprint_2017-09-21

1830 2017-11-11: Print version (16) for MiP2017/MitoEAGLE conference in Hradec Kralove

1831 *Phase 2* Mitochondrial respiratory states and rates: Building blocks of mitochondrial physiology Part 1

1832 http://www.mitoeagle.org/index.php/MitoEAGLE_preprint_2018-02-08

1833 • 2018-02-08 – (44+45 Versions up to 2018-10-25)

1834 *Phase 3* Submission to a preprint server: [BioRxiv](https://www.biorxiv.org/)

1835 *Phase 4* Journal submission

1836 CELL METABOLISM, aiming at indexing by *The Web of Science* and *PubMed*.

1837

1838

1839 S2. Authors

1840

1841 This manuscript developed as an open invitation to scientists and students to join as co-authors, to provide a
1842 balanced view on mitochondrial respiratory control and a consensus statement on reporting data of mitochondrial
1843 respiration in terms of metabolic flows and fluxes.

1844 Co-authors are added in alphabetical order based upon a first draft written by the corresponding author, who
1845 edited all versions. *Co-authors confirm to have read the final manuscript, possibly have made additions or*
1846 *suggestions for improvement, and agree to implement the recommendations into future manuscripts, presentations*
1847 *and teaching materials.*

1848 We continue to invite comments and suggestions, particularly if you are an early career investigator adding
1849 an open future-oriented perspective, or an established scientist providing a balanced historical basis. Your critical
1850 input into the quality of the manuscript will be most welcome, improving our aims to be educational, general,
1851 consensus-oriented, and practically helpful for students working in mitochondrial respiratory physiology.

1852 To join as a co-author, please feel free to focus on a particular section, providing direct input and references,
1853 and contributing to the scope of the manuscript from the perspective of your expertise. Your comments will be
1854 largely posted on the discussion page of the MitoEAGLE preprint website.

1855 If you prefer to submit comments in the format of a referee's evaluation rather than a contribution as a co-
1856 author, we will be glad to distribute your views to the updated list of co-authors for a balanced response. We would
1857 ask for your consent on this open bottom-up policy.

1858

1859

1860 S3. Joining COST Actions

1861

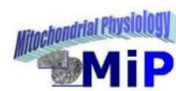
1862 • CA15203 MitoEAGLE - http://www.cost.eu/COST_Actions/ca/CA15203

1863 • CA16225 EU-CARDIOPROTECTION - http://www.cost.eu/COST_Actions/ca/CA16225

1864 • CA17129 CardioRNA - http://www.cost.eu/COST_Actions/ca/CA17129



Mitochondrial respiratory states and rates:



Building blocks of mitochondrial physiology

Part 1 - www.mitoeagle.org/index.php/MitoEAGLE_preprint_2018-02-08

Gnaiger E^{1,2}, corresponding author
355 co-authors, MitoEAGLE Working Group

¹Medical University Innsbruck
²Oroboros, Innsbruck, Austria

Aims Clarity of concept and consistency of nomenclature facilitate effective transdisciplinary communication, education, and ultimately further discovery.

Adhering to uniform standards and harmonizing the terminology concerning mitochondrial respiratory states and rates will support the development of databases of mitochondrial respiratory function in cells, tissues, and species.

Summary Recommendations on coupling control states and rates are focused on studies with mitochondrial preparations.

Fig. 1: Respiration is defined by O₂ flux balance.

Fig. 2: OXPHOS analysis is based on the study of mt- preparations. Metabolic fluxes measured in defined coupling and pathway control states provide insights into the meaning of cellular respiration.

Fig. 3: Interpretation of respiratory rates depends critically on appropriate normalization.

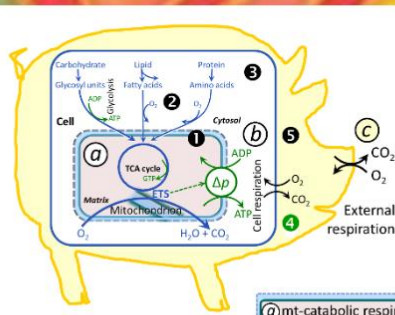
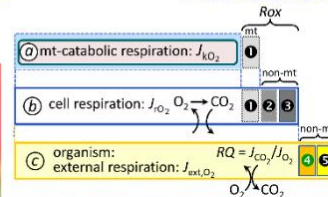


Figure 1. From mitochondrial to external respiration

Mitochondrial (mt) respiration is the oxidation of fuel substrates (electron donors) and reduction of O₂ catalysed by the electron transfer system, ETS:

- a** mt-catabolic respiration, excluding
- 1** mt-residual oxygen consumption, *Rox*.
- b** Total cellular O₂ consumption, including mt-*Rox*,
- e** non-mt catabolic *Rox*, particularly by peroxisomal oxidases, and
- 9** non-mt *Rox* unrelated to catabolism.

- c** External respiration, including
- 3** aerobic microbial respiration, and
- 5** extracellular O₂ consumption.



MIPart by Odra Noel



Figure 2. Respiratory states (ET, OXPHOS, LEAK) and corresponding rates (E, P, L)

Net OXPHOS-capacity, *P-L*, and excess capacity, *E-P*.

Table 1. Coupling states and residual oxygen consumption in mitochondrial preparations in relation to respiration- and phosphorylation-flux, *J_{kO₂}* and *J_p*, and protonmotive force, Δp . Coupling states are established at kinetically-saturating concentrations of fuel substrates and O₂.

State	<i>J_{kO₂}</i>	<i>J_p</i>	Δp	Inducing factors	Limiting factors
LEAK	<i>L</i> ; low, cation leak-dependent respiration	0	max.	proton leak, slip, and cation cycling	<i>J_p</i> = 0: (1) without ADP, <i>L_s</i> ; (2) max. ATP/ADP ratio, <i>L_r</i> ; or (3) inhibition of the phosphorylation-pathway, <i>L_{only}</i>
OXPHOS	<i>P</i> ; high, ADP-stimulated respiration	max.	high	kinetically-saturating [ADP] and [P _i]	<i>J_p</i> , by phosphorylation-pathway; or <i>J_{kO₂}</i> by ET-capacity
ET	<i>E</i> ; max., noncoupled respiration	0	low	optimal external uncoupler concentration for max. <i>J_{O₂E}</i>	<i>J_{kO₂}</i> by ET-capacity
ROX	<i>Rox</i> ; min., residual O ₂ consumption	0	0	<i>J_{O₂Rox}</i> in non-ET-pathway oxidation reactions	inhibition of all ET-pathways; or absence of fuel substrates

Figure 3. Normalization of rate

A: Cell respiration is normalized for (1) the experimental **Sample** (flow per object, mass-specific flux, or cell-volume-specific flux); or (2) for methodological reasons for the **Chamber** volume.

B: **Flow per cell** [amol O₂ s⁻¹ cell⁻¹] is flux per chamber volume, *J_v* [nmol O₂ s⁻¹ L⁻¹], divided by cell concentration in the chamber, *N_{cell}*/V [cells L⁻¹], which is **Number** analysis. In **Structure** analysis, aerobic cell performance is mt-quality (mt-specific flux, e.g., per citrate synthase, CS) times mt-quantity, or mt-function times mt-structure.



MitoEAGLE
Join
COST Action CA15203

Funded by the Horizon 2020 Framework Programme of the European Union

www.mitoeagle.org/index.php/MitoEAGLE

COST Action CA15203 MitoEAGLE

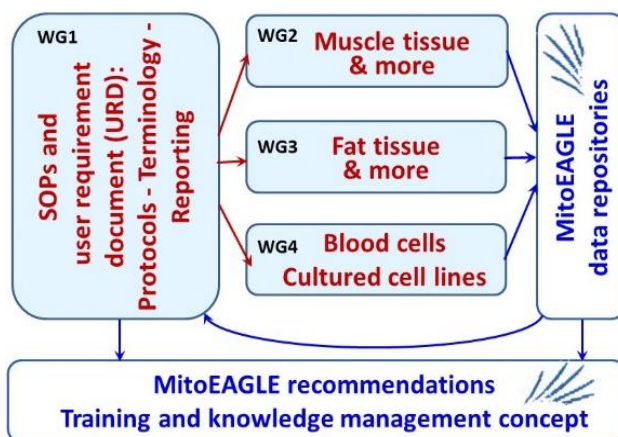
Evolution Age Gender
Lifestyle Environment



Mission of the global MitoEAGLE network

in collaboration with the Mitochondrial Physiology Society, MiPs

- Improve our knowledge on mitochondrial function in health and disease with regard to Evolution, Age, Gender, Lifestyle and Environment
- Interrelate studies across laboratories with the help of a MitoEAGLE data management system
- Provide standardized measures to link mitochondrial and physiological performance to understand the myriad of factors that play a role in mitochondrial physiology



Join the COST Action MitoEAGLE - contribute to the quality management network.



More information:
www.mitoeagle.org



Funded by the Horizon 2020 Framework Programme
of the European Union

1866

